Energy Migration and Trapping in a Spectrally and Spatially Inhomogeneous Light-Harvesting Antenna

Oscar J. G. Somsen, Frank van Mourik, Rienk van Grondelle, and Leonas Valkunas*

Department of Physics and Astronomy, Free University of Amsterdam, De Boelelaan 1081, 1081 HV, Amsterdam, The Netherlands; and the *Institute of Physics, A. Gostauto 12, 2600 Vilnius, Lithuania

ABSTRACT In this paper, we analyze the process of excitation energy migration and trapping by reaction centres in photosynthesis and discuss the mechanisms that may provide an overall description of this process in the photosynthetic bacterium *Rhodospirillum (Rs.) rubrum* and related organisms. A wide range of values have been published for the pigment to pigment transfer rate varying from less than 1 ps up to 10 ps. These differences occur because the interpretation of trapping measurements depend on the assumptions made regarding the organization of the photosynthetic system. As we show, they can be reconciled by assuming a spatially inhomogeneous model where the distance of the reaction center to its surrounding pigments is larger than the pigment-pigment distances within the antenna. We estimate their ratio to be 1.7–1.8.

The observed spectral inhomogeneity (at low temperature) of the photosynthetic antenna has resulted in various models. We demonstrate that the excitation kinetics can be modelled at all temperatures by assuming an inhomogeneous distribution of spectral shifts for each pigment. A transition temperature can be distinguished where the effects of spectral inhomogeneity become apparent and we discuss the ranges above (e.g., room temperature), around (e.g., 77K) and below (e.g., 4K) this temperature. Although the basic model is the same in all cases, the dominant mechanism differs in each range. We present explicit expressions for the exciton lifetime in the first two cases and demonstrate that at both temperatures the transfer rate from the light-harvesting antenna to the special pair of the reaction center is the rate-limiting step. Furthermore we demonstrate that at all temperatures a finite number of functional "levels" can be distinguished in the spectral distribution. At high temperature all pigments can be considered spectrally identical and only one level is needed. In the intermediate range a blue-shifted fraction is necessary. At low temperature a third redshifted fraction must be introduced.

I. INTRODUCTION

In photosynthesis the light-harvesting antenna (LHA) is responsible for the absorption of solar energy and its transfer to a specialized pigment-protein complex, the reaction center (RC), where the excitation energy is converted into a charge separation. During the past few decades this process has been investigated in a variety of photosynthetic systems, with complex spectroscopic and structural properties and increasingly complicated models have been developed to explain the dynamics of excitation transfer and trapping (Bay and Pearlstein, 1963; Robinson, 1967; Knox, 1977; Shipman, 1980; Pearlstein, 1982; Kudzmauskas et al., 1983; Valkunas, 1986; Valkunas et al., 1986; Jean et al., 1989; Fetisova, 1990; Skala and Kapsa, 1989; Skala and Jungwirth, 1989; Källebring and Hansson, 1991; Pearlstein, 1992).

Many kinetic studies have been performed at room temperature (RT) but this gives limited information about excited state kinetics within the longest wavelength absorption band of the LHA, because this band is typically always near thermal equilibrium and only overall trapping is observed. To obtain information on migration within the antenna, techniques such as singlet-singlet annihilation and depolarization experiments have been performed.

Additional information has been obtained from measurements at liquid nitrogen (77K), or liquid helium (4K) temperatures (Freiberg et al., 1987; van Grondelle et al., 1987; Godik et al., 1988; Visscher et al., 1989; Freiberg et al., 1989; Knox and Lin, 1988; Wittmershaus, 1987, Lyle and Struve, 1991; Werst et al., 1992; Timpmann et al., 1991). At these temperatures, spectral differences between various components of the photosynthetic system become apparent because a "downhill relaxation" occurs from blue- to red-shifted pigments. The observed kinetics are multiexponential and depend on the wavelengths of excitation and detection. This potentially gives information about migration within the LHA.

Similar kinetics have been observed in a variety of organisms. We focus on the photosynthetic purple bacterium *Rhodospirillum (Rs.) rubrum* which is among the best studied systems. It contains a single antenna species: B875 or LH1. This is built up from heterodimers of α- and β-polypeptides, and each $\alpha\beta$-pair binds one B875 bacteriochlorophyll *a* (BChl *a*) dimer (Visschers et al., 1991; van Mourik et al., 1991). The LH1 to RC stoichiometry is fixed to about 24 BChl *a* (12 dimers) per RC.

If the temperature is lowered to 77K or below, the longest-wavelength absorption band of the LHA shows the characteristics of a system with more than one spectral form. In addition to the 60-ps absorption/emission decay that is observed at room temperature, shorter (1–10 ps) lifetimes are

Received for publication 8 September 1993 and in final form 2 February 1994

Address reprint requests to Rienk van Grondelle at the Department of Physics and Astronomy, Free University Amsterdam, 1081 HV Amsterdam, The Netherlands.

0006-3495/94/05/1580/17 $2.00

present. At short emission/absorption wavelengths ultrafast absorption depolarization and increase of excited state absorption indicate <1-ps excitation transfer processes (van Grondelle et al., 1987; Pullerits et al., submitted for publication). If the absorption/emission is monitored in the low-energy wing of the spectrum a risetime of a few picoseconds is observed upon shorter wavelength excitation. At 4K the rise slows down with increasing wavelength (Timpmann et al., 1991). At this temperature a much longer (±600 ps) lifetime suggests the presence of LHA pigments with excited state energies lower than that of the RC.

Models for energy migration

Various models have been used to understand the multi-exponential kinetics in the longest wavelength band of *Rs. rubrum*. A common feature is that the single pigment type occurs in at least two spectral forms (Valkunas et al., 1991), induced by differences in environment. At present at least two conceptual frames exist; In the first, the LHA is arranged as an energetic funnel around the RC with a minor fraction (10–20%) of red-shifted BchI *a* pigments (B896) close to it and a major fraction of blue-shifted pigments (B875) at the periphery (Seely, 1973; van Grondelle et al., 1988), so that energy transfer is directed to the RC. This theory successfully explains 4K fluorescence polarization (Kramer et al., 1984), 77K time-resolved absorption (van Grondelle et al., 1988; Sundström et al., 1986; Bergström et al., 1989) and fluorescence kinetics (Shimada et al., 1989), and annihilation (van Grondelle et al., 1988; van Grondelle, 1985; Borisov et al., 1982; Vos et al., 1986; Deinum et al., 1989; Deinum, 1991).

The second hypothesis originates from the observation that at 4K as at 77K the fluorescence kinetics depends continuously on the emission wavelength (Freiberg et al., 1987; Godik et al., 1988; Freiberg et al., 1989; Timpmann et al., 1991), which demonstrates the presence of more than two spectral components. Therefore, it has been suggested that the major absorption band is inhomogeneously broadened, meaning that each pigment has a random spectral shift, independent of all other pigments and of its spatial position within the LHA. This is supported by measurement of low temperature polarized fluorescence excitation spectra on isolated small complexes (van Mourik et al., 1992, Visschers et al., 1993). Obviously, these models reflect opposing views of the energy trapping process and are therefore of interest to be compared in detail.

Recently Pullerits and Freiberg (1991, 1992) simulated the energy transfer and trapping process in a spectrally inhomogeneous LHA. The relative probability to find a particular spectral form is given by the ground state absorption spectrum of the LHA. The remaining parameters in this model are the lattice spacing a between neighboring pigments (actually the ratio of the Förster radius R_0 and a) and the homogeneous bandwidth of the pigments. The latter can be deduced from the temperature dependence of the absorption spectrum. With this model, Pullerits and Freiberg explained the 77K experimental data. With the same physical constants, they obtained a quantitative fit to the observed kinetics at 300K (Pullerits and Freiberg, 1991) and could qualitatively explain the data at 4K (Pullerits and Freiberg, 1992).

Pullerits and Freiberg interpreted the 10-ps decay phase that is observed at low temperature as excitation equilibration dynamics which is correlated to the excitation hopping time τ_{hop} between neighboring pigments. They concluded that the energy trapping by the RC is migration-limited (or at least close to that) and that τ_{hop} is approximately 10 ps even at room temperature (RT). This gives an excitation diffusion radius close to the dimensions of a photosynthetic unit. This slow hopping requires that the spacing parameter a is rather large.

This estimate for τ_{hop} is in conflict with the value extracted from singlet-singlet annihilation (van Grondelle, 1985; Vos et al., 1986; Deinum et al., 1989; Deinum, 1991; Valkunas, 1989; Trinkunas and Valkunas, 1989; den Hollander et al., 1983; Bakker et al., 1983) and depolarization measurements (van Grondelle et al., 1987), which indicate ultrafast energy migration (τ_{hop} <1 ps at RT). In this case the radius of excitation diffusion is rather large, covering several photosynthetic units. Modelling this process on a lattice determined by only one lattice constant a (which is smaller than the value determined by Pullerits and Freiberg) predicts that the excitation lifetime is trap-limited (Bakker et al., 1983).

In this paper we present the outline of a model that may synthesize the opposing views of: 1) two- (or more) level versus inhomogeneous distribution of the pigments in the LHA, 2) a funnel model with directed- versus a random model with undirected energy transfer, 3) slow- versus fast hopping, and 4) migration-limited versus trap-limited kinetics.

This model includes structural and spectral inhomogeneity. First of all, we consider that the distance of the RC to its neighboring pigments is not necessarily identical to that between LHA pigments so that two spatial parameters appear that determine the energy migration. A second type of structural inhomogeneity is included (Kudzmauskas et al., 1983; Valkunas, 1986; Fetisova, 1990), because the LHA itself consists of closely packed pigment-protein complexes, in which the average distance between pigments is much smaller than that between pigments of different complexes. Finally, we assume that the spectral distribution of the pigments of the LHA is inhomogeneous.

Note that the inclusion of both structural and spectral inhomogeneity does not make the model unnecessarily complicated because they can be studied independently. At RT the spectral distribution only influences the very first part (<1 ps) of the excitation decay kinetics. In the remainder, only structural inhomogeneity will be observed. Only upon lowering the temperature does the spectral inhomogeneity become increasingly visible.

Although the model that we present is the same at all temperatures, the parameters that determine the kinetics differ with temperature. In Section II we calculate the excitation

lifetime in a structurally inhomogeneous LHA. This result is used in Section III to analyze RT kinetics. In Section IV, we discuss the kinetics at intermediate temperatures (e.g., 77K), where the influence of spectral inhomogeneity is not strong and can be analyzed using perturbation approaches. In Section V, we discuss the kinetics at low temperature (e.g., 4K) where a perturbation approach is not possible. Instead the elimination of "uphill" energy transfer allows us to distinguish functional pigment pools. In Section VI we investigate the implications of these models for the interpretation of annihilation experiments.

A common factor at all temperatures is that spectral inhomogeneity can be modelled by a finite number of levels. We show that at RT, the LHA can be modelled as a one-level system, at 77K as a two-level system with high energy states that decay rapidly into a population of low energy states resonant with the RC, and at 4K as a three-level system with a small fraction of the pigments below the RC.

II. ENERGY MIGRATION IN A STRUCTURALLY INHOMOGENEOUS LIGHT-HARVESTING SYSTEM

In principle, the analysis of the energy trapping process in a system with N pigments using a Master equation involves the diagonalization of a $N \times N$ matrix (see Eq. A1 in the Appendix) which gives N decay times. A mixture of nonidentical systems gives even more decay times.

However, experimental kinetics rarely contain more than a one or a few lifetimes. This is because the excitation distribution evolves to a thermal equilibrium in a number of rapid exponential processes and then decays monoexponentially. The decay time related to this last process is the excitation lifetime under consideration. Its behavior can be analyzed with random walk theory (Knox, 1977; Pearlstein, 1982; Kudzmauskas et al., 1983; Valkunas, 1986). If the LHA is not too small ($\geq$10 pigments/RC) the trapping by the RC can be modelled as a local perturbation of a trapless system. The resulting expression has two terms (see also Appendix and Pearlstein (1982), and Kudzmauskas et al. (1983))

$$\tau = \tau_{trap} + \tau_{mig} \qquad \text{(II1)}$$

where τ_{trap} is the lifetime of the excitation if the equilibrium distribution is not distorted by the presence of the RC, while τ_{mig} accounts for this distortion. The trapping rate $1/\tau_{trap}$ is proportional to the probability of population of the RC and its relaxation rate $1/\tau_{rel}$. In case of a homogeneous LHA, the population of each pigment equals $1/N$ (where N is the number of pigments per RC including the RC). Therefore

$$\tau_{trap} = N\tau_{rel}. \qquad \text{(II2)}$$

The migration term τ_{mig} is the average "first passage" time for an excitation to the RC. It is determined by two factors; The transfer (hopping) time τ_{hop} between neighboring pigments which depends on the distance a between them, and the size and structure of the LHA, accounted for by the structure function $f_d(N)$ (Pearlstein, 1982; Kudzmauskas et al., 1983; Valkunas, 1986)

$$\tau_{mig} = \frac{1}{2} N f_d(N) \tau_{hop}. \qquad \text{(II3)}$$

For one-dimensional systems, $f_d(N)$ is equal to 1, while for various LHA with different dimensions d it is of the same order of magnitude as can be seen in Fig. 1.

The influence that structural inhomogeneity around the RC has on the excitation lifetime is reflected in the value of τ_{rel}. In a structurally homogeneous model, τ_{rel} is equal to the charge separation time γ^{-1} of the isolated RC. If, however, the distance between the special pair of the RC and its neighboring pigments significantly differs from the distance between pigments within the LHA, the delivery rate W_1 to the RC and the detrapping rate W_2 (see Fig. 2) are different from the hopping rate. In that case a perturbation approximation (Pearlstein, 1982; Valkunas, 1986) yields

$$\tau_{rel} = \frac{W_2}{W_1}\gamma^{-1} + \frac{W_1^{-1} - \tau_{hop}}{z}, \qquad \text{(II4)}$$

where z is the number of pigments connected to the RC (the coordination number).

The spatial inhomogeneity influences both W_1 and W_2 but the ratio W_2/W_1 in the first term reflects detailed balance

$$\frac{W_1}{W_2} = e^{-\Delta E_{RC}/k_B T} \qquad (\Delta E_{RC} = E_{RC} - E_{LHA}), \qquad \text{(II5)}$$

which depends only on the excited state energies of the RC and the LHA. The dependence on spatial inhomogeneity is in the second term of Eq. II4 and accounts for the change in population of the RC. Due to its migration nature it can be included in τ_{mig}, as done by Pearlstein (1982). But, since this factor is influenced by the presence of the RC we include it here. In this way τ_{mig} describes the behavior of the LHA and τ_{trap} the presence of the RC.

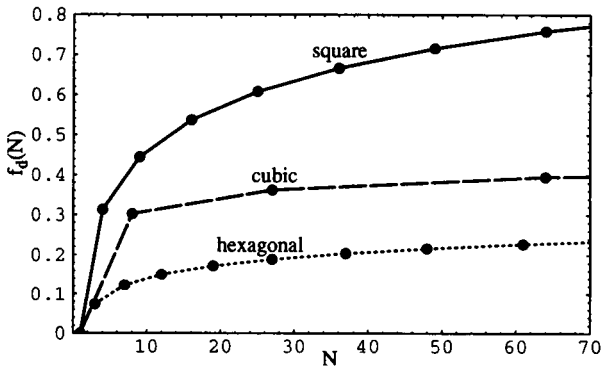

FIGURE 1 The structure function $f_d(N)$ for an LHA organized as a two-dimensional square lattice (*solid*), a three-dimensional cube (*dashed*), or a two-dimensional hexagonal lattice (*dotted*). N is the total number of pigments per RC. The structure function $f_d(N)$ gives the relation between τ_{hop}, N and the migration time as in Eq. II3. Adapted from Kudzmauskas et al. (1983).

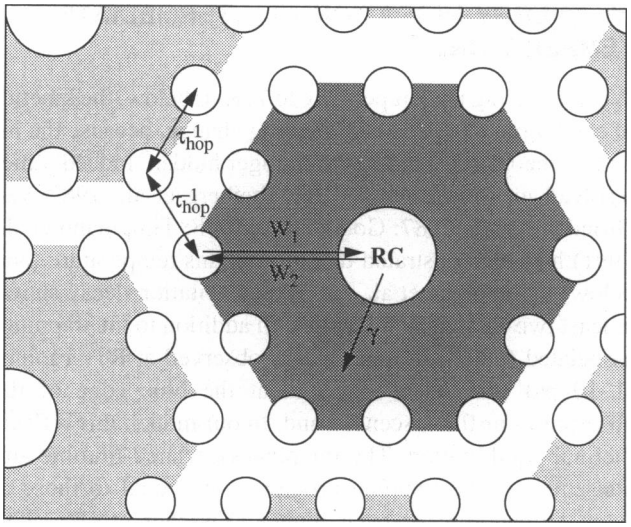

FIGURE 2 A hexagonal LHA-RC model for excitation migration at RT. Each photosynthetic unit contains 1 RC- and 12 LHA-sites and is surrounded by six other units. Transfer between neighboring sites, either within one unit or between neighboring units, takes place with the hopping rate τ_{hop}^{-1}, while W_1 and W_2 are the rates of transfer to and from the RC, respectively. The charge separation rate is γ.

Influence of structural inhomogeneity within the LHA

Additional structural inhomogeneity within the LHA can influence the excitation lifetime. The LHA pigments are organized in pigment-protein complexes. The energy migration in such a complex is not always purely incoherent. It has been shown that in LH1 of photosynthetic purple bacteria dimerization of the pigment molecules takes place (Visschers et al., 1991; van Mourik et al., 1991). Second, even if the pigments within a complex are not excitonically coupled, the transfer between pigments within a complex is faster than the inter-complex transfer so that a second (much faster) timescale of migration appears. Moreover, the migration between the pigment-protein complexes deviates from the Förster mechanism when the size of the complexes is comparable to the intercomplex distance a.

We account for this inhomogeneity, by treating pigment-protein complexes as single sites, as done in the analysis of singlet-singlet annihilation measurements (Valkunas, 1986; van Grondelle, 1985; Valkunas, 1989; Trinkunas and Valkunas, 1989; den Hollander et al., 1983). The parameter τ_{hop} reflects the hopping between these sites. The interpretation of kinetic parameters in such a model is only possible in combination with other experimental data; although τ_{hop} is determined by the intercomplex distance a, this value cannot be directly calculated with Förster's equation.

III. ENERGY MIGRATION AT ROOM TEMPERATURE

The low temperature (FWHM) width of the 880-nm LH1 absorption band of *Rs. rubrum* is approximately 20 nm (258 cm^{-1}). This is an upper limit to the inhomogeneous bandwidth. If we assume it to be temperature-independent and compare it to k_BT which is 212 cm^{-1} at RT, we see that all but the most extreme spectral inhomogeneities are "turned off" at this temperature so that only structural inhomogeneity remains and the theory of the previous paragraph may be applied. This implies that, with additional information, the RT kinetics inform us about the structural inhomogeneity.

From fluorescence experiments (Freiberg et al., 1987; Godik et al., 1988; Freiberg et al., 1989; Timpmann et al., 1991; Valkunas et al., 1991) we find the excitation lifetime $\tau = 60$ ps. In order to estimate the migration time we use $\tau_{hop} = 0.65$ ps for transfer time between sites as determined from the singlet-singlet annihilation experiments (van Grondelle, 1985; Valkunas, 1989; Trinkunas and Valkunas, 1989; Bakker et al., 1983). The pigment:RC ratio is 24:1 but $N = 13$, since we assume that the basic building block is a dimer (Visschers et al., 1991; van Mourik et al., 1991). We evaluate the case of a two-dimensional hexagonal model for the LHA (see Fig. 2) for which $f_d(N) \approx 0.15$ (see Fig. 1). We set $z = 6$ because not all pigments are likely to have a favorable transition-dipole for transfer to the RC. For comparison we also evaluate a square model ($f_d(N) = 0.50$) with $z = 4$, although no simple structure can be found with $N = 13$.

Equation II3 gives $\tau_{mig} = 0.6$ and 2.1 ps, respectively. Thus, the excitation lifetime is trap-limited and $\tau_{rel} = 4.6$ and 4.5 ps, respectively, from Eq. II2. This is slower than the charge separation (2.8 ps) observed in isolated RCs (Martin et al., 1986; Fleming et al., 1988). We conclude that delivery and detrapping rates (W_1, W_2) play a role and Eq. II4 has to be applied.

We calculate first the ratio of W_2 and γ by comparing the fluorescence yield upon excitation of the LHA with that upon selective excitation of the RC (e.g., for *Rs. rubrum* at the 800-nm absorption band of monomeric BChl *a* pigments of the RC). The ratio $1/m = zW_2/(\gamma + zW_2)$ is experimentally found to be about ⅓ (Timpmann et al., 1993) or even less (Wang and Clayton, 1971; Danielius and Razjivin, 1988; Otte et al., 1993). So we continue our calculation for $m = 3$ (and $m = 5$). The above mentioned equation can be rewritten as $zW_2/\gamma = 1/(m - 1)$ and thus $(zW_2)^{-1} = 5.6$ ps (11.2 ps). Substitution in Eq. II4 gives $(zW_1)^{-1} = 3.1$ ps (3.7 ps). In the case of the hexagonal model, $W_1^{-1} = 18.7$ ps (22.4 ps), while the square model gives $W_1^{-1} = 13$ ps (16 ps) and $W_2^{-1} = 22.4$ ps (44.8 ps).

In both cases the estimates for W_1^{-1} and W_2^{-1} are much larger than τ_{hop}, which confirms that they limit the excitation lifetime. This conclusion has been confirmed by measurements on site-specific mutants (Beekman et al., accepted for publication), where it was found that the excitation lifetime in the LHA-RC depends only weakly on the charge separation time.

We can relate these kinetic parameters to the structure of the light-harvesting system. From detailed balance (Eq. II5) we find that the average separation between the excited state energy levels of the LHA and the RC is $\Delta E_{RC} = -170$K

(−320K) for both hexagonal and square lattice cases, indicating that it is redshifted by 9 nm (17 nm). This by itself, causes an accumulation of excitations on the RC and thus faster trapping.

The accumulation is however more than compensated by the slow delivery and detrapping rates. If we interpret this in terms of distances, the distance for energy transfer from the LHA to the RC is larger than that between sites within the LHA. If Förster's equation is applicable and W_1^{-1}/τ_{hop} is 25–30, their ratio is 1.7–1.8.

Although this result clearly suggests that the delivery of excitations to the RC is slow with respect to hopping, an actual interpretation in terms of structure requires additional information. However, it correlates well with the ring-like structures observed for LHA-RC core complexes of *Rhodopseudomonas (Rps.) viridis* (Miller, 1982) and more recently for *Rps. marina* (Meckenstock et al., 1992) and *Rs. molischianum* (Germeroth L., Boekema E., Michel H., private communication). In these structures the 12 BChl *a* dimers are situated on a ring surrounding the RC, with an outer diameter 10 nm and an inner diameter of 6 nm. The average dimer-dimer distance is then about 2 nm, while the average distance to the center of the structure, where the special pair is located is about 4 nm. Note that the estimates of W_1 and W_2 depend also on other factors, such as the coordination number z.

These complications, however, do not invalidate the implication of these results for the modelling of energy migration. If we wish to understand both the trapping kinetics (Pullerits and Freiberg, 1991) and the annihilation results it is plausible to assume a structural inhomogeneity so that the trapping, and more in particular the delivery to the RC is the rate-limiting step. The conclusion that the RC is slightly redshifted from the LHA so that it works as a weak funnel is in accordance with its function as a trap.

We also consider the case of closed RCs. In that case the excitation lifetime is τ_c = 200 ps (Timpmann et al., 1991; Valkunas et al., 1991; Sundström et al., 1986). The increase is most likely due to the change of transfer rates between LHA pigments and the RC. Because the quenching of the excitation in a closed RC is very fast, W_1^c becomes even more limiting and Eq. II4 can be simplified to

$$\tau_c = \frac{N}{zW_1^c}. \qquad \text{(III1)}$$

In the case of $N = 13$ and $z = 6$, $1/W_1^c = 92$ ps. If we interpret this using Förster's theory, it implies that the overlap of the emission spectrum of the LHA and the absorption spectrum of the RC decreases by a factor of 5 which is confirmed by the bleaching of the B890 band of the isolated RC when it changes from the "open" to the "closed" state (Meiburg, 1985). W_2^c is of no importance in the case of closed RCs.

Now that we have found an effective structural model with two scaling parameters, we investigate the influence of spectral inhomogeneities at lower temperature.

IV. ENERGY MIGRATION AT INTERMEDIATE TEMPERATURE

When lowering the temperature to 77K or below, the kinetics of excitation migration and trapping change, because the inhomogeneous broadening is no longer hidden. Indeed, time-resolved measurements at 77K (Freiberg et al., 1987; van Grondelle et al., 1987; Godik et al., 1988; Timpmann et al., 1991) have demonstrated that around this temperature (and below) (Timpmann et al., 1991) the excitation decay shows at least two-exponential kinetics. In addition to the trapping-associated (60 ps) lifetime that is observed at RT, a minor (1–10 ps) component is found at the blue edge of the absorption- or fluorescence band. In our model, this reflects thermal equilibration. The trapping-associated lifetime and consequently the trapping efficiency are equal to those at room temperature or even higher (Visscher et al., 1989; Bergström et al., 1989).

Excitation kinetics in spectrally and spatially inhomogeneous structures can be modelled numerically (Parson and Kopelman, 1985; Movaghar et al., 1986; Burshtein, 1985; Gochanour et al., 1979). But, in the intermediate temperature range where the effect of spectral inhomogeneity on the kinetics is small, it can be approximated with perturbation-like theories. In this section we estimate the equilibration time which is related to the homogeneous (σ_h) and the inhomogeneous (σ_{inh}) bandwidth (we use FWHM bandwidths throughout the article). Furthermore, we discuss the influence of spectral inhomogeneity on the trapping process. The main question is: does the excitation delivery to the RC remain the rate-limiting step or does this change upon lowering the temperature? This is under debate because decreasing spectral overlap may cause a slower excitation transfer.

However, before we investigate energy migration in spectrally inhomogeneous LHA, we first consider the influence of spectral difference on the transfer rate $W(E, E', r)$ between individual pigments, i.e., when donor and acceptor have different excited state energies, E and E' respectively. It also depends on the distance r between them. We follow an empirical approach (Parson and Kopelman, 1985),

$$W(E, E', r) = \tau_{hop}^{-1}\left(\frac{a}{r}\right)^s \exp\left(\frac{E - E'}{2k_BT}\right)\phi(E - E'), \qquad \text{(IV1)}$$

where τ_{hop} is the temperature-dependent transfer rate between pigments with the same spectral shift (i.e., for $E = E'$) that are one lattice distance (a) apart, while $\phi(E - E')$ models the dependence on the (difference between) their energy levels. The Boltzmann factor is included to symmetrize ϕ; i.e., detailed balance is satisfied if and only if $\phi(E - E') = \phi(E' - E)$. For Förster transfer, $s = 6$ and $\phi(E - E')$ is the symmetrized spectral overlap of donor emission and acceptor absorption normalized to $\phi(0) = 1$. In the high temperature case, it is a gaussian shaped function of width $\sqrt{2}\sigma_h$.

The Boltzmann factor causes a blueshift of this gaussian. The transfer between two pigments is fastest, according to Eq. IV1, if $E = E' + \sigma_h^2/(8 \ln 2k_BT)$. The shift should be

approximately equal to the (homogeneous) Stokes' shift (S), i.e.,

$$\sigma_h^2 \approx 8 \ln 2 S k_B T. \tag{IV2}$$

This is correct in the high temperature limit (Agranovich and Galanin, 1982; Osad'ko. 1979).

Thermal equilibration

The 1–10-ps decay on the blue side of the fluorescence band is due to thermal equilibration. If the temperature is not too low, the equilibrium distribution extends over a large fraction of the pigments, and the equilibration is almost complete after the first transfer step. The fact that this takes considerably longer than the <1-ps hopping time at RT can be understood with the Förster mechanism, because the initially excited pigment is blueshifted with respect to the center of the inhomogeneous band, so that the spectral overlap with most of its neighbors is unfavorable.

To calculate the decay of the number of excitons surviving on the initially excited pigment at energy level E, given by the diagonal Green's function of the Master equation $G^s(E, t)$, in a spectrally inhomogeneous LHA, we have to average over all possible environments of this pigment. To establish this, we use a spectrally random molecular array model for the LHA (Parson and Kopelman, 1985; Movaghar et al., 1986; Burshtein, 1985); $G^s(E, t)$ can be calculated if we ignore back-transfer. This is allowed at sufficiently low temperature, because we consider a donating pigment at the blue edge of the absorption band,

$$G^s(E, t) = \prod_i \int\int f(E')\rho_i(\bar{r}) e^{-W(E, E', r)t}\, dE'\, d\bar{r}, \tag{IV3}$$

where $f(E')$ gives the inhomogeneous distribution of the spectral shift, which is the same for all pigments and $\rho_i(\bar{r}_i)$ the distribution of the positions of the pigments surrounding the donor. We assume that these distributions are independent.

We must now implement a spectral and structural model for the LHA in order to evaluate Eq. IV3. As to the spectral model, we assume that the inhomogeneous and homogeneous bands are gaussians of width σ_{inh} and σ_h, respectively. We discuss two different structural models. First, the structural inhomogeneity may be included by modelling the LHA as a glass with ρV acceptors (ρ is the density of LHA pigments) distributed independently over a volume V. In the limit of a large volume Eq. IV3 simplifies to (Agranovich and Galanin, 1982)

$$G^s(E, t) = \exp\left[-\rho \int dE' f(E') \int d\bar{r}(1 - e^{-tW(E, E', r)})\right]. \tag{IV4}$$

This approximation can also be used at higher temperatures where the survival time is influenced by back-transfer, by renormalizing with substitutions: $\rho \to \rho/2$ and $W \to 2W$ (Burshtein, 1985).

With the abovementioned assumptions, the integrals in Eq. IV4 can be evaluated and the result simplifies if the spectral forms have relatively narrow homogeneous bands, so that $\sigma_h \ll \sigma_{inh}, k_B T$ in that case,

$$G^s(E, t) = e^{-(t/\tau_d)^{d/s}} \tag{IV5}$$

$$\tau_d = \tau_{hop} \Big/ \left(\pi^{d/2} \sqrt{\frac{2s}{d}} \frac{\Gamma(1 - d/s)}{\Gamma(1 + d/2)} \frac{\sigma_h}{\sigma_{inh}} e^{-(E - E_0/0.6\sigma_{inh})^2}\right)^{s/d}$$

where Γ is the gamma function and d the dimension of the LHA.

The main advantage of the glass model is that $G^s(E, t)$ can be calculated analytically in a spectrally inhomogeneous LHA. However, it overestimates the equilibration rate, because it ignores the size of the pigment-protein complexes and therefore the exclusion zone around the donating pigment. To investigate this we evaluate Eq. IV5 for a two-dimensional LHA: $d = 2$, $s = 6$ with $E = E_0 + 0.6\sigma_{inh}$ and find: $\tau_d^{-1} = 56\, \tau_{hop}^{-1}(\sigma_h/\sigma_{inh})^3$. In this time, $G^s(E, t)$ decays by a factor e^{-1}. The same decay time can be calculated for a square lattice model at high temperature (i.e., $\sigma_h \gg \sigma_{inh}$) and is equal to $4.7\, \tau_{hop}^{-1}$ (or $4\, \tau_{hop}^{-1}$ if only nearest-neighbor transfer is considered). Apparently the two models are incompatible at high temperature. The discrepancy must be caused by the exclusion zone. Consequently, the glass model is in this form inadequate for studying the dependence of the equilibration rate on σ_h and we have to consider an alternative.

A second structural model for the LHA can be formed by ignoring the structural inhomogeneity and considering it as a lattice (i.e., $\rho_i(\bar{r}) = \delta(\bar{r} - \bar{r}_i)$). Now, Eq. IV3 breaks down to a product of integrals which do not allow an analytical evaluation, but are readily calculated numerically. We carried out this calculation for a range of homogeneous bandwidths and excitation wavelengths. Equation IV1 was used for the transfer rates with Gaussian bands for the homogeneous and inhomogeneous distributions.

Some results are shown in Fig. 3. The decay of G^s is not monoexponential. It shows a fast initial decay which occurs in those LHA, where the donating pigment has a favorable spectral overlap with its neighbors. This is followed by a slower decay. And for $\sigma_h < 0.4\sigma_{inh}$, decay times occur that are even longer than the time range of the simulation. However, unlike the glass model, the decay rate does converge to $4.66\, \tau_{hop}^{-1}$ for large σ_h.

Because of the multiexponentiality, the curves can not be fitted with a simple one- or two-exponential decay. However, a fit with a two-exponential decay is possible when we include an offset (rms <0.2%). The latter corresponds to a decay time much longer than the fit window ($20\, \tau_{hop}$). The faster of the two fitted decay times is in all cases faster than $1.8\, \tau_{hop}$. This coincides with the initial (<1 ps) equilibration processes which are not included in our analysis. Therefore the experimentally observed 1–10-ps decay on the blue side

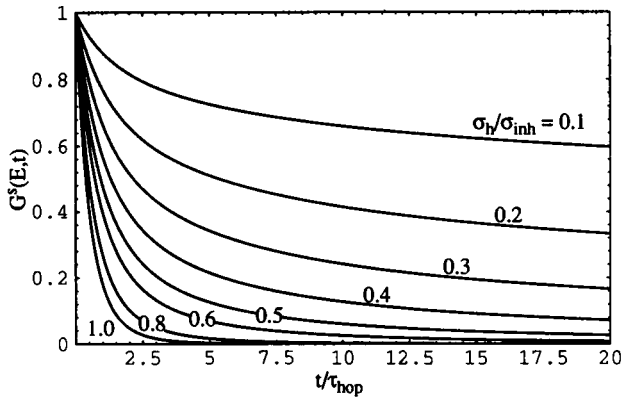

FIGURE 3 Simulation of the decay of the number of excitons that survive on the initially excited pigment on the blue side of the band (at $E = E_0 + 0.6\sigma_{inh}$). A spectrally inhomogeneous square LHA model was used with various homogeneous bandwidths as indicated in the plot. Time is relative to τ_{hop}.

of the fluorescence band can be compared to the slower of the two fitted decay times (τ_2).

Fig. 4 shows τ_2 as a function of σ_h/σ_{inh} for various blue-shifted donating pigments. It demonstrates that decay from the initially excited pigment has a slow component that slows down with increasing blueshift of this pigment. Slow decay is also found if the donating pigment is in the center of the LHA absorption band, but only if σ_h is very small. However, this does not contribute much to the experimentally observed signal, because the accepting pigments have in that case almost the same spectrum as the donating pigment. We therefore estimate the equilibration time by considering donating pigments with an energy $E \approx = E_0 + 0.6\sigma_{inh}$.

In order to estimate σ_h from this result we also have to account for the temperature dependence of the transfer time τ_{hop} between pigments with the same spectral shift. The spectral overlap for such pigments decreases proportional to

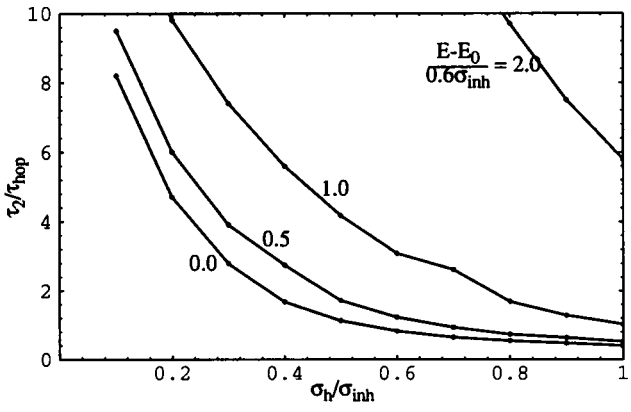

FIGURE 4 Decay time (relative to τ_{hop}), as a function of homogeneous bandwidth, of the number of excitons surviving on the initially excited pigment. Results were obtained by fitting to simulations with an inhomogeneously broadened square LHA model and are shown for various blueshifts ($E - E_0$) of the initially excited pigment as indicated in the plot.

$\sigma_h \sim T^{1/2}$ (see Eq. IV2) or more if $\sigma_h \lesssim S$. Thus τ_{hop} is approximately two times slower than the RT value (i.e., 1 ps). For the observed 1–10-ps decay on the blue side of the fluorescence band, τ/τ_{hop} = 1–10 so that σ_h/σ_{inh} = 1–0.2.

Apparently a thermal equilibration that lasts up to 10 τ_{hop} can be explained by a decreasing transfer rate from the initially exited pigment, provided that the homogeneous bandwidth is small. In such a model it is necessary to consider a large number of accepting pigments in the LHA, because transfer to nearest neighbors can become slower than transfer to other pigments. It should be noted that other mechanisms can also explain a slow equilibration component. It has been suggested that the 10-ps equilibration time results from slow equilibration between local wells in the LHA (van Mourik et al., 1993; Pullerits et al., submitted for publication).

Excitation lifetime

The effect of spectral and structural inhomogeneity on the excitation lifetime τ can be estimated with Eq. II1. It has two terms τ_{mig} and τ_{trap}. The influence of inhomogeneities can be considered on each of these separately.

First we investigate the influence on τ_{mig} as can be seen from Eq. II3, this is either through a change of the hopping rate or the number of steps to the RC. If all transfer rates in the LHA change with some factor (due to decreasing spectral overlap) τ_{mig} changes with the same factor. But differentiation of the rates causes a complicated effect which is incorporated in the structure function $f_d(N)$. It may be argued that this function decreases with decreasing temperature, because the restriction of the excitons to the red-shifted pigments implies that the excitations reach the RC in fewer steps. However, we will see in the following that this is not the case.

The structure function of an LHA can be expressed in terms of the Green's function $G(\lambda)$ of the Master equation of an LHA without traps (Kudzmauskas et al., 1983; Valkunas et al., 1986) even in the spectrally inhomogeneous case (Appendix B). Therefore, the perturbation of $f_d(N)$ can be evaluated by considering the perturbation of $G(\lambda)$ which can be done by expanding it as a power series in $\beta = 1/k_BT$ (see Appendix C)

$$f_d(N) = f_d^0(N) + \left(\frac{\sigma_{inh}}{\sigma_h}\right)^2 \frac{1}{2} \sum_{\substack{i \\ a \in \Omega}} \left(\frac{G_{0i}^0 - G_{ai}^0}{\tau_{hop}}\right)^2 + O(\beta^2), \tag{IV6}$$

where Ω is the set of nearest neighbors to site 0. The temperature dependence of this expression is included by the temperature dependence of σ_h, which we take from Eq. IV2. To first order the perturbation of $f_d(N)$ depends on the square of the ratio of σ_{inh}/σ_h. Because the perturbation is a sum of squares, the structure function increases with decreasing temperature. This may physically be explained by the decrease in symmetry as demonstrated in Fig. 1. The G_{ij}^0 refer to a spectrally homogeneous LHA and Eq. IV6 and can be evaluated for various LHA. For a 3 × 3 square LHA :

$f_d(N) = 0.22 + 0.22(\sigma_{inh}/\sigma_h)^2$ (Eq. C8) and for a hexagonal LHA ($N = 7$) $f_d(N) = 0.12 + 0.12(\sigma_{inh}/\sigma_h)^2$ (Eq. C9). From continuation up to higher order, it seems that this approximation is correct at least for $\sigma_h \geq \sigma_{inh}$.

From the perturbation of $f_d(N)$ we can evaluate τ_{mig}, but we have to take the temperature dependence of τ_{hop} (see Eq. II3) into account. Due to spectral overlap this increases proportional to $\sigma_h^{-1} \sim T^{-1/2}$ (Eq. IV2) or more if $\sigma_h \lesssim S$. Therefore, τ_{mig} increases considerably and the excitation lifetime need not be as strongly limited by τ_{trap} as at RT.

As the second part of the excitation lifetime we consider the perturbation of τ_{trap} (Eq. II4). The first term is determined by the ratio W_1/W_2, which after averaging depends on the mean value of ΔE_{RC} (see Eq. II5). The second term depends on the distance between RC and LHA through W_1 and contains no essential temperature dependence.

We can now reconsider the analysis that we have done at RT. If we assume that the migration time does not increase too strongly, the excitation decay remains trap-limited and $\tau_{rel} \approx 4.5$ ps. The absence of any appreciable changes in the trapping component at 77K (Freiberg et al., 1987; Visscher et al., 1989), and in the case of closed RC down to 4K (Godik et al., 1988; Timpmann et al., 1991) confirms that it is dominated by the second term of Eq. II4. Consequently, the first term can be ignored at all temperatures. This is only possible if $\Delta E_{RC} \lesssim -300$K (17 nm) which places the RC at the red edge of the LHA longest wavelength absorption band. This implies that at 77K, $W_1/W_2 > 50$ so that the first term of Eq. II4 can be ignored. It is however possible that a decrease of this term when decreasing the temperature from RT to 77K, is compensated by an increase of τ_{hop} in the second term. We estimate $(zW_1)^{-1} \approx 4.5$ ps so that $W_1^{-1} = 18$ ps for a square ($z = 4$) LHA structure and 27 ps for a hexagonal ($z = 6$) structure.

Two level models

The considerations in this section, and the presence of only two lifetimes in kinetic measurements at 77K, suggest that, at this temperature, two pools can be distinguished in the inhomogeneous distribution of pigments, as indicated in Fig. 5. The pigments on the blue side are represented in level 1. Trapping from this level can be ignored as long as the excitations transfer at a reasonable rate to the larger fraction of red-shifted pigments that are represented in level 2. This transfer corresponds with thermal equilibration, and its rate (k_{12}) is related to σ_h and σ_{inh} as in Fig. 4. The trapping takes place from level 2, and its rate may be approximated by $k_{RC}^{-1} \approx ((z/N)W_1)^{-1} \approx 60$ ps, while $\bar{k}_{RC}^{-1} \approx (zW_2)^{-1} > 300$ ps.

We also consider the case of closed RCs. These quench excitons even faster so that $\bar{k}_{RC}^{c}$ can be ignored. Consequently $1/k_{RC}^{c}$ is equal to the experimentally observed excitation lifetime $\tau_c = 270$ ps (Freiberg et al., 1987; Godik et al., 1988; Timpmann et al., 1991).

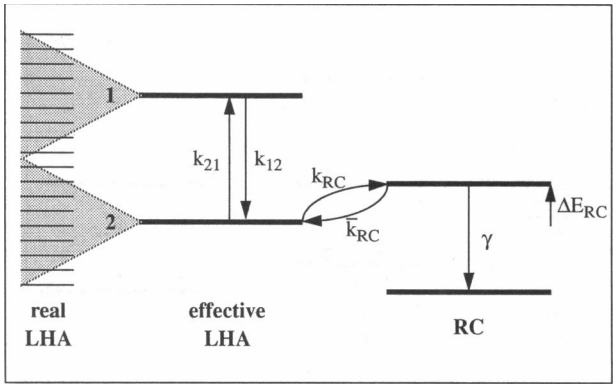

FIGURE 5 Effective excitation trapping scheme at 77K. Two effective levels are distinguished in the continuous inhomogeneous distribution of excitation energy levels in the LHA. Level 2 contains the red-shifted pigments that are well populated in thermal equilibrium. Transfer to and from the RC takes place with effective rates k_{RC} and $\bar{k}_{RC}$, respectively. Level 1 contains the blue-shifted pigments that transfer their excitations to level 2 with rate $k_{12} \gg k_{21}, k_{RC}$. Therefore, effectively no transfer takes place from level 1 to the RC.

V. ENERGY MIGRATION AT LOW TEMPERATURE

At temperatures far enough below the width of the spectral inhomogeneity, only downhill transfer occurs. At such temperatures, the spectral inhomogeneity of the LHA is most pronounced. Indeed, time-resolved experiments at 4K (Timpmann et al., 1991) show an additional ≈600 ps lifetime on the red side of the fluorescence band that was not observed at 77K or RT. Other changes are the decrease of the charge separation yield to 60% and the 5-fold increase of the fluorescence yield (Rijgersberg et al., 1980). These phenomena may be explained by the pigments that are red-shifted beyond the RC and act as additional traps.

A perturbation approach to calculate kinetics of the LHA at this temperature is not possible. However, the occurrence of only downhill transfer also causes a simplification. Following the model developed at 77K, we suggest that three pigment pools must be distinguished in the inhomogeneous distribution as is illustrated in Fig. 6. Levels 1 and 2 have the same function as in the 77K model although their detailed characteristics are different. Level 3 is introduced to model the longest wavelength spectral forms (Movaghar et al., 1986). Between these levels only downhill transport takes place. Therefore we can set up the kinetic equations and solve them algebraically. Within this model, the populations n_i of level i satisfy

$$\frac{dn_1}{dt} = -k_1 n_1 \qquad \frac{dn_2}{dt} = \mu_2 k_1 n_1 - k_2 n_2$$
$$\frac{dn_3}{dt} = \mu_3 k_2 n_2 + \mu_1 k_1 n_1 - k_3 n_3 \tag{V1}$$

where k_i is the effective rate of transfer away from level i and μ_i gives the quantum yield of various transitions.

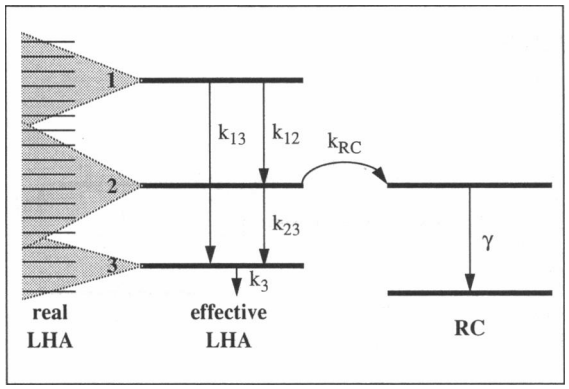

FIGURE 6 Effective excitation trapping scheme at 4K. Analogous to the 77K scheme (Fig. 5). However, a third level is added that contains the redmost pigments which are populated at thermal equilibrium. Level 2 contains the pigments that are near to resonant with the RC. No trapping takes place from level 1 because excitations are transferred much faster to levels 2 and 3. The only decay from level 3 is spontaneous relaxation, k_3, because all other transfer is "uphill." Kinetic parameters have the same meaning as in Fig. 5.

They are related to the effective kinetic parameters shown in Fig. 6 by

$$k_1 = k_{13} + k_{12} \qquad k_2 = k_{23} + k_{RC}$$
$$\mu_1 = \frac{k_{13}}{k_1} \qquad \mu_2 = \frac{k_{12}}{k_1} \qquad \mu_3 = \frac{k_{23}}{k_2} \qquad \mu_{RC} = \frac{k_{RC}}{k_2}. \tag{V2}$$

Decay rate k_3, which is the sum of fluorescence rate k_f and radiationless decay takes place from all three levels. We only include it in level 3 because that is the only level where it influences the kinetics.

The solution of Eq. V1 with the initial conditions $n_1(0) = n_0$, $n_2(0) = n_3(0) = 0$, representing excitation on the blue side of the absorption band, is

$$n_1 = n_0 e^{-k_1 t} \qquad n_2 = \frac{n_0 \mu_2 k_1}{k_1 - k_2}(e^{-k_2 t} - e^{-k_1 t})$$
$$n_3 = \frac{n_0 \mu_1 k_1}{k_1 - k_3}(e^{-k_3 t} - e^{-k_1 t}) + \frac{n_0 \mu_2 k_1}{k_1 - k_2} \tag{V3}$$
$$\times \left[\frac{\mu_3 k_2}{k_2 - k_3}(e^{-k_3 t} - e^{-k_2 t}) - \frac{\mu_3 k_2}{k_1 - k_3}(e^{-k_3 t} - e^{-k_1 t})\right].$$

In addition we can evaluate the yields of charge separation (μ_{CS}) and fluorescence (μ_f)

$$\mu_{CS} = \mu_2 \mu_{RC} \qquad \mu_f = \frac{\mu_1 + \mu_2 \mu_3}{k_3} k_f + \frac{\mu_2}{k_2} k_f + \frac{k_f}{k_1}. \tag{V4}$$

We can now estimate the kinetic parameters. First, consider that level 3 contains less than one pigment per RC, because if that is not be the case it traps a larger fraction of the excitations. The fraction of level 2 pigments is therefore much larger and thus $k_{13} \ll k_{12}$ so that $k_{12}^{-1} = k_1^{-1} = 10$ ps. Equation V4 reduces to $\mu_{RC} = \mu_{CS} = 0.6$. If we assume that $k_{RC}^{-1} = 60$ ps the same value as at RT and 77K we find $k_{23}^{-1} = 90$ ps and $k_2^{-1} = 36$ ps. Since k_3^{-1} is known to be 600 ps we can estimate the ratio of 4K and RT fluorescence, if we assume that k_f is the same for both temperatures. We find a ratio of 5.3 which is near the experimentally observed ratio of 5. Our first assumption is confirmed by this outcome because it may be argued that $k_{13} \approx k_{23} \ll k_{12}$. The kinetic parameters can be solved with the assumption $k_{12} = k_{23}$ instead of $k_{13} \ll k_{12}$ but the result is almost the same. The traces resulting from Eq. V3, with the values of the effective rate constants as discussed above are presented in Fig. 7.

The same analysis may also be applied for closed RCs. Using the value $k_{RC}^c = 270$ ps that we found from the analysis at 77K we obtain $/k_2^c = 68$ ps. The resulting traces are shown in Fig. 8.

The excitation decay from levels 1 and 3 is properly included in this model. But the trapping associated component $1/k_2^c$ is somewhat faster than the experimentally found intermediate kinetics of 100–200 ps (Timpmann et al., 1991). However, it should be noted that the parameters $1/k_{RC}$ and k_{RC}^c in this calculation are the average trapping times from level 2 which may be slower than their RT value, because some additional slow transfer takes place from level 2 pigments that are slightly redshifted with respect to the RC. This explains the minor discrepancy with the observed kinetics. Note also that the rise-time of the redmost n_3 emission is not necessarily the same as the decay time of n_2 since it is excited both from n_1 and n_2.

These estimates determine the kinetic behavior upon excitation of the shortest wavelength pigments. However, it can be extended to different excitation wavelengths; when the excitation wavelength is increased, the rate k_1 of the fastest kinetic component increases as can be seen from Fig. 4 and becomes indistinguishable from the equilibration process. This is consistent with experimental data (Freiberg et al., 1987; Godik et al., 1988; Timpmann et al., 1991). Therefore, this model can also be used with excitation of level 2 instead of 1.

The kinetic parameters that we estimated above are related to the structural and spectral composition of the LHA-RC system. However, the relation is not straightforward. If we

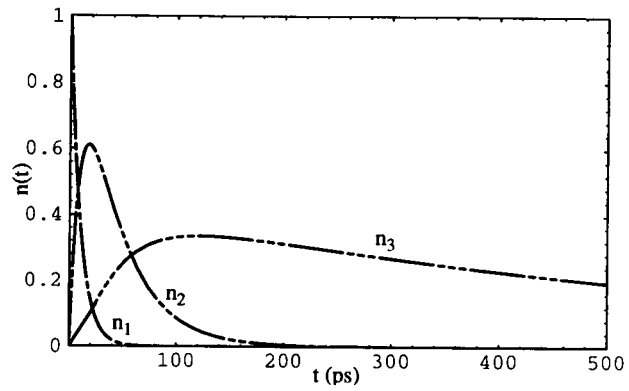

FIGURE 7 Excitation kinetics for an inhomogeneously broadened LHA with open RC at 4K. $n_i(t)$ gives the excitation population in level i as defined in Fig. 6. Parameters are taken from the text and defined in Eq. V2: $\mu_1 = 0$, $\mu_2 = 1$, $\mu_3 = 0.4$, $\mu_{RC} = 0.6$, $k_1^{-1} = 10$ ps, $k_2^{-1} = 36$ ps, $k_3^{-1} = 635$ ps.

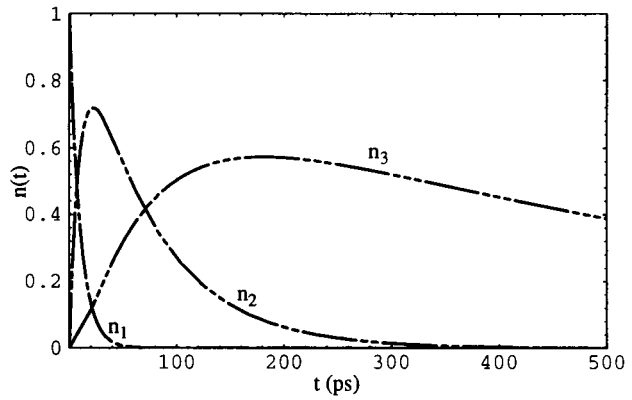

FIGURE 8 Excitation kinetics for an inhomogeneously broadened LHA with closed RC at 4K. $n_i(t)$ gives the excitation population in level i as defined in Fig. 6. Parameters are taken from the text and defined in Eq. V2: $\mu_1 = 0$, $\mu_2 = 1$, $\mu_3 = 0.75$, $\mu_{RC} = 0.25$, $k_1^{-1} = 10$ ps, $k_2^{-1} = 68$ ps, $k_3^{-1} = 635$ ps.

wish to interpret the parameters we must apply further simplifications and assume that these levels can be identified and are randomly scattered, that each level is constantly in thermal equilibrium, that uphill energy transfer does not occur, and that downhill transfer between any two pigments occurs with a fixed rate k. In that case the transfer rates depend on the fractions f_i of the pigments that are in each level i. Any pigment has z neighbors, so that the transfer from level j to i is given by $k_{ji} = zf_ik$. This leads us to conclude that $f_2/f_3 = k_{12}/k_{23} = 9$ so that $f_3 < 0.1$. If an appreciable number of pigments is in f_1 the number will be even less.

Apparently, only a small fraction of the pigments is redshifted beyond the RC. This means that the RC itself must be redshifted with respect to the centre of the inhomogeneous LHA absorption band. If we further simplify the model by considering the case that the RC itself is not inhomogeneously broadened, this leads us to the estimate that the RC must be at least redshifted by more than 0.54 σ_{inh} or approximately 11 nm with respect to the LHA. This agrees with the result we obtained at 77K.

VI. SINGLET-SINGLET ANNIHILATION

Because of the inhomogeneously broadened nature of photosynthetic systems, as discussed in the previous sections, the singlet-singlet annihilation process differs from that of homogeneous systems. The distribution of singlet excitations over the LHA is not homogeneous and will depend on the excitation and detection wavelength. Therefore, the analysis of annihilation measurements reveals additional information about these processes. In this section we provide a qualitative analysis with the models discussed above.

The fluorescence quantum yield dependence on excitation light intensity has been measured at RT (van Grondelle, 1985; Vos et al., 1986; Valkunas, 1989; Trinkunas and Valkunas, 1989; den Hollander et al., 1983; Bakker et al., 1983; Paillotin et al., 1979) and the analysis with annihilation theory for homogeneous systems gives a migration rate τ_{hop} as well as the average domain that is visited by an excitation. As discussed, the kinetics in the LHA of *Rs. rubrum* at this temperature resemble that of a spectrally homogeneous structure and, therefore, the application of such an analysis is justified. A model for small domains (compared to the excitation diffusion radius) (van Grondelle, 1985; Vos et al., 1986; den Hollander et al., 1983; Bakker et al., 1983; Paillotin et al., 1979) as well as a many-particle approach (Valkunas, 1989; Trinkunas and Valkunas, 1989) give qualitatively similar conclusions. It should be noted that the quantum yield analysis is not a very sensitive method. Essentially higher sensitivity has been obtained by analysing the change of the kinetics (Valkunas, 1989; Kudzmauskas et al., 1985, 1988, 1986). It has been determined that $\tau_{hop} = 0.65$ ps (Valkunas, 1989; Trinkunas and Valkunas, 1989) and that the number of pigments in the photosynthetic unit is $N = 13$.

At lower temperature, spectral inhomogeneity plays a role. In annihilation experiments at low temperature (Vos et al., 1986; Deinum et al., 1989; Deinum, 1991) the threshold intensity depends on the detection wavelength. This has been analyzed within the B875–B896 (two-level) concept (Deinum et al., 1989), and it was concluded that mini domains exist of more than 10 B896 pigments organized around a few RCs. However, if a third level is present, representing low energy pigments that act as additional traps, the analysis has to be repeated.

In the following we describe a mechanism for singlet-singlet annihilation at 4K. The LHA can not be considered homogeneous, but the relevant theory may still be applied if we can account for the spectral inhomogeneity by adapting the excitation diffusion coefficient. At asymptotically large time intervals the diffusion coefficient can indeed still be defined (Parson and Kopelman, 1985; Movaghar et al., 1986; Burshtein, 1985). However, annihilation predominantly occurs at shorter times, when the concentration of excitations is high (Valkunas, 1989; Kudzmauskas et al., 1988). Therefore, this only works at low intensity of the excitation light, close to the threshold where annihilation starts. Since there is no general theory for annihilation in inhomogeneous systems this is the only analysis that we can use to provide qualitative estimates.

Let us therefore consider singlet-singlet annihilation on the basis of the three level model that we presented in Fig. 6. In this model the excitations reside for a finite time (k_i^{-1}) in each level. During this time they migrate within the level with a diffusion coefficient D_i (which is different for each level) and thus can annihilate. The radius of the average diffusion domain of an excitation is:

$$R_i = \sqrt{2dD_ik_i^{-1}}, \qquad \text{(VI1)}$$

where d is the dimension of the system. We assume that at the threshold intensity on the average, one pigment (or at least a fixed number) is excited in each domain with radius R_i which is a rough, but reasonable approximation. In this way, the threshold intensity at various wavelengths directly relates to the diffusion radius and thus to the diffusion coefficient in the corresponding level.

An essential condition for this model is that at the threshold intensity of each level, no appreciable annihilation in higher levels occurs. But even if this condition is satisfied it is a simplified picture. For instance, the excitation of each level does not occur instantaneously. Part of the photons directly excite the level under consideration but others are supplied from higher levels at a longer timescale. Furthermore, annihilation by an excitation from a different level is not taken into account. However, the large differences in lifetime, spectral separation (Timpmann et al., 1991) and annihilation threshold intensity (Visscher et al., 1989; Freiberg et al., 1989; Knox and Lin, 1988) suggest that this approximation is reasonable.

Level 3 has a different position in this model. Because it contains a very small fraction of the pigments, it is below the percolation threshold and the pigments are unconnected. The diffusion coefficient D_3 is zero and almost no annihilation takes place within this level. Instead, efficient annihilation takes place with excitations from level 2.

We can now analyze the annihilation measurements. From time-resolved fluorescence data (Timpmann et al., 1991) we conclude that the fluorescence at 905 nm corresponds mainly to level 1, and that at 918 nm to levels 2 and 3. The fluorescence quantum yield has been monitored at these wavelengths at 4K and RT for LHA with closed RCs (Vos et al., 1986; Deinum et al., 1989; Deinum, 1991). The analysis at 905 nm shows that the threshold intensity increases 10-fold when the temperature is decreased to 4K from which we conclude that the diffusion domain at 4K is ten times smaller than at RT. However, if we take into account that the excitation lifetime at RT (closed RCs) is 200 ps with respect to $k_1^{-1} = 10$ ps, it turns out that D_1 is approximately equal to the excitation diffusion coefficient at RT.

This is consistent with our model. Apparently the diffusion is hardly hindered by restriction of the excitations to level 1 so this level must contain a major fraction of the pigments. This agrees with the relatively long time (10 ps), compared to the hopping time, that excitations reside in level 1. There is no sign of the hopping rate being much lower at 4K than at RT as would be the case when it is an activation like process. On the contrary, the slightly higher diffusion coefficient suggests that the hopping rate may even increase.

At 918 nm the threshold intensity is five times lower than at 905 nm, which satisfies the condition for applying our model to level 2, but it is still half an order of magnitude higher than at RT. If we do not consider annihilation by excitations in level 3, the diffusion radius $R_2^2 \approx 3.2\ R_1^2$ is larger than in level 1, but this is mainly caused by the longer lifetime ($k_2^{-1} = 170$ ps) only. This results in $D_2 \approx 0.2D_1$. If we also consider annihilation by excitations in level 3, the estimate for D_2 becomes even smaller. Apparently, diffusion in level 2 is hindered. This is either because excitations are restricted to a part of the lattice since level 1 sites are no longer accessible or if the level 2 pigments form local wells because the transfer takes place between non-nearest neighbors.

In combination with the analysis of 4K kinetics in the previous section, and under the simplifying assumptions at the end of that section, this indicates that a large fraction (>50%) of the pigments belong to level 1, while 90% of the remaining pigments belongs to level 2, and only a tiny fraction belongs to level 3.

VII. SUMMARY AND DISCUSSION

Structural inhomogeneity

In this paper we have discussed the basic mechanisms that determine the excitation transfer and trapping kinetics in spatially and spectrally inhomogeneous LHA. The analysis is initiated by kinetic measurements in the absorption bands of *Rs. rubrum* (Timpmann et al., 1991). At RT the trapping is described by a monoexponential process of 60 ps, which should be compared to the fast (<1 ps) transfer within the LHA that has been found from singlet-singlet annihilation and polarized time-resolved absorption (van Grondelle et al., 1987; Sundström et al., 1986; Bakker et al., 1983). Our analysis shows that the RT situation can be explained if the excitation decay rate is limited by the rate of delivery (W_1) of excitations to the RC. The analysis indicates that this remains true down to 4K.The slow delivery may be explained by assuming a spatial inhomogeneity in the LHA-RC complex. We estimate that the distance from the LHA sites to the special pair in the RC is 1.7–1.8 times larger than between sites within the LHA, probably as a result of the bulky shape of the RC.

A second type of spatial inhomogeneity that we have considered is the organization of BChl molecules in clusters. It has been shown that at least dimerization takes place upon the formation of the LHA (Visschers et al., 1991; van Mourik et al., 1991). The coherent interaction may also contribute to the decrease of fluorescence lifetime from 5.5 ns in free chlorophyll (Karukstis, 1991) to the 600-ps lifetime of the longest component at 4K. In our model the BChl clusters are treated as single sites.

Spectral inhomogeneity

The appearance of additional components in time-resolved fluorescence and absorption at 77K and below strongly suggests the presence of more than one spectral form (Freiberg et al., 1987; van Grondelle et al., 1987; Godik et al., 1988; Timpmann et al., 1991). So far the experimental data could for a large part be explained on the basis of the two-level model, B875–B896, with the redmost fraction closely associated to the RC. Recent site-selected (van Mourik et al., 1992) and time-resolved (Timpmann et al., 1991) fluorescence experiments at 4K have shown that this model must be extended and should contain at least three, but possibly many spectral species. We assume a model with a continuous distribution of excited state energy levels that allows us to understand the excited state kinetics over the whole temperature range. Our analysis shows that at RT the inhomogeneity is hidden by homogeneous broadening and only the abovementioned spatial inhomogeneity has to be considered.

The thermal equilibration which has a time scale of 1–10 ps at 77K can be related to the survival time on the initially excited blue-shifted pigments. We estimate from this that at this temperature the homogeneous bandwidth of the individual pigments is smaller than the width of inhomogeneous distribution ($\sigma_h/\sigma_{inh} = 0.2$–1) which supports our model. The excitation lifetime is equal or possibly slightly smaller than that observed at RT. This suggests that deviation from the room temperature behavior is small and low order approximations can be used to "correct" for the inhomogeneity. A perturbation approach leads us to the conclusion that energy migration is slower than a RT, but that the excitation lifetime remains limited by the rate of delivery W_1 to the RC. A conceptual model requires two functional groups in the spectral distribution (see Fig. 5). Within each level, the excitations are in equilibrium. The transfer rates between levels depend on Förster transfer rates between individual pigments as well as on the average structural organization.

The kinetics at 4K can be understood by introducing a third level (see Fig. 6) of redshifted pigments that act as additional traps. If the photosynthetic domains are small, this minor fraction contains those pigments that are most redshifted in their domain and also more redshifted than the RC. On the other hand, if the domains are very large, it contains the pigments whose excited state energy is a local minimum. Note, that in the first case some domains may not contain such a redshifted level 3 pigment. Once excited, the excitation will not escape from a level 3 pigment. At 77K this level is indistinguishable from level 2. The existence of this level explains not only the kinetics but also the observed 40% decrease in charge separation and the 5-fold increase in fluorescence yield observed for *Rs. rubrum* (Rijgersberg et al., 1980).

We can not exclude the possibility of very slow trapping from level 3 as proposed by (Kleinherenbrink et al., 1992). This raises the question whether excitations are trapped from level 2 pigments as we assume or from level 3. In the latter model the trapping is 10-fold slower. So, if we assume that the radiative lifetime is the same at 4K as at RT the 5-fold increase in fluorescence yield implies that no more than 44% of the excitations can have such a long lifetime. By comparing this to the 60% charge separation yield observed at this temperature, trapping from level 3 pigments is ruled out. This question may be decided by directly observing the rate of oxidation of the special pair in the RC.

Our analysis of kinetics at RT, 77K and 4K indicates that the average energy level of the RC is 10–17 nm below that of the LHA pigments. Note that we are discussing here the location of the zero-phonon transitions of the LHA and RC. Since the zero-phonon transition has (in these two cases) a negligible contribution to the spectrum, the observed absorption spectrum is blue-shifted relative to the "zero-phonon-spectrum" by (roughly) the "half-width" of the phonon-wing. The absorption spectra of the B880 band of the LHA and the special pair of the RC are rather similar, and no relative spectral shift is observed. This can be explained because the RC spectrum is largely homogenous, $\sigma_h > 2^*\sigma_{inh}$, (Johnson et al., 1989), whereas in the LHA inhomogeneous broadening prevails; $\sigma_h < \sigma_{inh}$ (van Mourik et al., 1992; Visschers et al., 1993). Therefore, though the absorption spectra appear similar, the zero-phonon-spectrum of the RC is significantly redshifted relative to that of the LHA.

The model allows a qualitative explanation of the steady-state emission spectra. The increasing Stokes shift upon lowering the temperature demonstrates that at 77K most of the fluorescence originates from mobile excitations in level 2, while at 4K emission occurs from excitations in level 3. This is supported by site-selected T-S spectra (van Mourik et al., 1992).

Approximations in our approach

The distinction of two functional pigment levels at 77K and three at 4K is a simplification which is partly inspired by the number of components found in transient fluorescence- and absorption measurements. There are however more arguments that support this view; multiexponential kinetics appears only when there is a large difference between thermal equilibrium and the initial distribution. If we consider only the excitations on a group of pigments with excited state energies close to each other (say within k_BT), the equilibrium within that group is established in a few steps. Moreover, the initial distribution is close to equilibrium already. Once equilibrium is established within each energetic level, only transfer between different levels has to be considered.

A consequence of this reasoning is that both the number of levels and the size of each level depends on temperature. Especially at 4K a larger number may be expected. For instance, in level 1 and 2 local traps are formed in which the excitation may be transiently localized for a few picoseconds before transfer to another (slightly lower) local minimum takes place. Thus, at some temperature the number of pigments in each level drops below the percolation threshold, they become largely unconnected and equilibration no longer occurs within each level. On the other hand, many of these levels have virtually indistinguishable kinetics as well as transient spectra. Therefore we group them in a few functional levels. The transfer rates between such levels may have to be renormalized.

We use a "nearest neighbor" approximation in most cases. This works well as long as each pigment has a neighbor to transfer to. However, for some pigments at the red edge of the absorption band of the LHA the transfer to all nearest neighbors is "uphill" and impossible at low temperature. For these pigments, transfer to non-neighbors has to be taken into account, albeit at a much lower rate. This is especially important for calculating the rate of diffusion in level 2, which is already hindered (in agreement with our analysis of annihilation measurements) because of the restriction to sites that are not occupied by level 1 pigments. If the percentage of level 2 pigments is low enough, these pigments are local traps and only long-distance transfer occurs between them. Level 3 pigments are sufficiently separated so that no transfer takes place between them. This agrees with the absence of

depolarization when exciting in the red wing of the LHA band (van Mourik et al., 1992).

The kinetics of a spectrally inhomogeneous system is essentially nonexponential. The equation for trapping at RT and 77K (Eq. II4) contains the mean values of ΔE_{RC} and W_1, but in fact this rate is different for each photosynthetic unit. Even if the kinetics of each individual unit contain a few exponentials, the experimentally observed kinetics reflects the average over all possible systems. The result may be nonexponential, for instance as described by Eq. IV5. This explains the presence of multiexponential kinetics (Timpmann et al., 1991) in the level which is in resonance with the RC (level 2 according to Fig. 6). However, there may be several causes that lead to a process that shows only a few-exponential phases in its decay like the appearance of a thermal equilibration or a rate-limiting step.

On the basis of our analysis, we can now compare the spectrally inhomogeneous model with the B880–B896 funnel model for the longest wavelength band of the LHA. Both models explain RT and 77K kinetics in much the same way and we have demonstrated that a random arrangement of the spectral forms does not necessarily slow down trapping. Fluorescence polarization (Kramer et al., 1984) and annihilation measurements (Deinum, 1991) at 4K have both been explained with the B880–B896 model but require mutually exclusive assumptions for the size of the B896 domain. This problem does not occur in the inhomogeneous model, because a different fraction of the spectral distribution is involved in the fluorescence polarization. The spectrally inhomogeneous model also explains excitation kinetics at 4K, which is not possible with the B880–B896 model. The fact that the spectral distribution can be represented by two spectral forms at 77K may explain the relative success of the B880–B896 model to explain experimental data.

Although our model is the same at all temperatures and applies to any spectrally inhomogeneous system, it is essential to distinguish three temperature ranges, each with a different analysis. These ranges are determined by the width (σ_{inh}) of the inhomogeneous spectral distribution. At "high" temperature, much larger than σ_{inh}, the system is always in thermal equilibrium and migration kinetics show no dependence on excitation and detection wavelength. All pigments can be considered to be of the same energy level. At "low" temperature, much smaller than σ_{inh} all migration kinetics depend essentially on the spectral distribution and three energy levels have to be distinguished within the inhomogeneous band. In between these two extremes, there is an "intermediate" temperature range, where a thermal equilibration is observed, the excitation lifetime depends mildly on the spectral distribution, and two energy levels can explain the observed kinetics.

This intermediate (or transition) temperature can be considered as a parameter which determines whether or not spectral inhomogeneity is observed. In general, it may be estimated from experimental data even if we consider that, apart from inhomogeneous broadening, additional small effects such as structural inhomogeneity or variations in the protein environment contribute to its value. In that case it is an empirical parameter which is not necessarily equal to σ_{inh}. This situation is analogous to the definition of the spatial parameter a as done in the room temperature model.

L. V. acknowledges a visitor-fellowship from the Dutch Organization for Scientific Research (NWO).
This work was supported by the NWO through the Dutch Foundation for Biophysics.

APPENDICES

In appendix A we give an overview of the kinetic equations for excitation transfer within a light-harvesting system and the Green's function formalism. In Appendix B we use this formalism to calculate the excitation lifetime in the presence of a trap. This is an extension of the result achieved earlier (Kudzmauskas et al., 1983; Valkunas et al., 1986) for homogeneous systems. In Appendix C we calculate how this lifetime is influenced by averaging over spectral inhomogeneity.

Appendix A: Overview of the Green's function formalism

The evolution of the excitation distribution in a light harvesting system is given by a Master equation,

$$\frac{d}{dt}a_n(t) = \sum_m H_{nm}a_m(t), \tag{A1}$$

where $a_n(t)$ is the probability of finding the excitation on the nth pigment. H_{nm} is the matrix that contains the rate constants: The non-diagonal entries H_{nm} give the transfer rate from mth pigment to the nth, while H_{nn} is negative and equal to the total rate of transfer away from the nth pigment plus its relaxation rate. The equation can be rewritten to an equation that is similar to the Schrödinger equation in operator form

$$\frac{d}{dt}\Psi(t) = H\Psi(t) \qquad \Psi(t) = \sum_n a_n(t)|n\rangle. \tag{A2}$$

The vector $|n\rangle$ corresponds to a state where the nth pigment molecule is excited and all others are in the ground state. The operator H is related to the matrix via $H_{nm} = \langle n|H|m\rangle$. We can apply the methods analogous to those developed for quantum mechanics, including perturbation theory. Let us therefore write

$$H = H^0 + U \tag{A3}$$

where H^0 is the rate matrix for some unperturbed system for which we can algebraically solve Eq. A1, while U is the perturbation caused by traps or spectral inhomogeneity. If U is small enough with respect to H^0, perturbation theory may be applied.

Special functions are available to characterize the solutions of a Master equation. We consider the Green's function as applied in Eq. IV6

$$G(\lambda) = (\lambda - H)^{-1}, \tag{A4}$$

the inverse of $\lambda - H$, where H is either a matrix or an operator as defined above and λ stands for "λ times the identity matrix." The Green's function has many applications. Amongst others, the excitation decay rates correspond to the singularities of $G(\lambda)$.

For H^0 we find the corresponding G^0. The relation between the two is readily checked to be given by Dyson's equation

$$G(\lambda) = G^0(\lambda) + G^0(\lambda)UG(\lambda). \tag{A5}$$

Appendix B: Excitation lifetime in a lattice with traps

We now use this equation to study the influence of traps on the excitation lifetime. In this case, $G^0(\lambda)$ corresponds to a trapless system which can be spectrally homogeneous for which case these results were earlier derived by (Kudzmauskas et al., 1983), or spectrally inhomogeneous. We assume it has one equilibrium state (fluorescence and other losses can simply be ignored and later added to the decay rate). This implies that $G^0(\lambda)$ is singular at $\lambda = 0$. In particular, the diagonal entry $G^0_{00}(\lambda)$ can be written as

$$G^0_{00}(\lambda) = \frac{a_1}{\lambda} + \frac{a_2}{\lambda - \lambda_2} + \cdots + \frac{a_N}{\lambda - \lambda_N}. \tag{B1}$$

Where $\lambda_2, \ldots, \lambda_N$ are the other eigenvalues H^0. The constant a_1 is the population of pigment 0 in the equilibrium state. In a spectrally homogeneous system $a_1 = 1/N$ but in other cases this is not necessarily true.

We assume a trap is present at pigment 0 with a decay rate γ. The $N \times N$ perturbation matrix U_{ij} has only one non-zero entry $-\gamma$ at $i = j = 0$. In this particular case Dysons's Eq. A5 simplifies considerably and gives an explicit equation for the diagonal entry $G_{00}(\lambda)$

$$G_{00}(\lambda) = \frac{G^0_{00}(\lambda)}{1 + G^0_{00}(\lambda)\gamma}. \tag{B2}$$

As mentioned above, any eigenvalue λ of the perturbed system corresponds to a singularity of $G(\lambda)$ and must therefore satisfy

$$G^0_{00}(\lambda)\gamma = -1. \tag{B3}$$

If the function $G^0_{00}(\lambda)$ is known, this equation allows us (in principle) to monitor the excitation decay rate as well as the other eigenvalues as a function of γ. At least in the case of $\gamma = 0$, they are equal to those of the trapless system.

Although this equation can not generally be solved, we can use it to obtain the excitation decay rate $-\lambda$ as a power series in γ. In order to achieve this, we split $G^0_{00}(\lambda)$ in a singular and a non-singular part by defining: $\bar{G}^0_{00}(\lambda) := G^0_{00}(\lambda) - a_1/\lambda$. $\bar{G}^0_{00}(\lambda)$ is a nonsingular, can be written as a power series around $\lambda = 0$ and therefore also as a power series around $\gamma = 0$. By substituting this into Eq. B3 we obtain

$$-\lambda = \frac{a_1\gamma}{1 + \bar{G}^0_{00}(\lambda)\gamma} = a_1\gamma[1 - \bar{G}^0_{00}(0)\gamma] + O(\gamma^3). \tag{B4}$$

Where we have to substitute only the constant term of the power series of $\bar{G}^0_{00}(\lambda)$ which is equal to $\bar{G}^0_{00}(0)$. The excitation lifetime $\tau = -1/\lambda$ is a singular function of γ and can be written as

$$\tau = \frac{1}{a_1\gamma} + \frac{1}{a_1}\bar{G}^0_{00}(0) + O(\gamma). \tag{B5}$$

If we compare this to Eq. 1 we find that

$$\tau_{trap} = a_1^{-1}\gamma^{-1} \quad \text{and} \quad \tau_{mig} = a_1^{-1}\bar{G}^0_{00}(0). \tag{B6}$$

More complicated local perturbations can be handled in a similar fashion.

Appendix C: Perturbation of Green's function by spectral inhomogeneity

We now study how this is influenced by spectral inhomogeneity. Note that from this point on, $G^0(\lambda)$ refers to a spectrally homogeneous system. We consider perturbations caused by inhomogeneous broadening. We only have to monitor a_1 and $G_{00}(\lambda)$ at λ close to 0, while properly accounting for the singular term. In particular the singular term in $a_1^{-1}\bar{G}_{00}(\lambda)$ is not perturbed (i.e., remains equal to $1/\lambda$). Therefore, we simply consider the perturbation of $G_{00}(\lambda)$ instead of $\bar{G}_{00}(\lambda)$.

Moreover, we are not dealing with just one perturbation U. In fact there are a large number of LHA systems in any sample, each with a different perturbation. The value of τ_{mig} is related to $G(\lambda)$ averaged over this distribution.

We find this average by considering that the perturbation entries U_{ij} depend on their turn on the energy levels E_i of the pigments in the LHA and the (inverse) temperature β ($= 1/k_BT$). The E_i are distributed independently, with identical distribution functions $f(E_i)$ which is related to the absorption spectrum of the LHA. The average of the Green's function is:

$$\langle G\rangle(\beta) = \int \cdots \int G(E_1, \ldots, E_N, \beta) f(E_1) \ldots f(E_N)\, dE_1 \ldots dE_N. \tag{C1}$$

Both G and $\langle G\rangle$ are functions on the parameter λ (see Eq. A4). But, because we continue our approach for a fixed value we leave it out of the equations below.

Naturally, G is a complicated function of the E_i and the averaging is generally impossible. This problem can be overcome by writing G as a power series in β for each value of the E_i. The coefficients of this series are functions of the E_i and may be averaged instead.

The constant term in this power series is equal to its value at $\beta \approx 0$ (i.e., high temperature). In that case the LHA is homogeneous and $G = G^0$. We calculate higher order terms in three stages; First we expand G as a power series in the entries U_{ij} up to nth order. These entries are a function of the E_i and β and we expand them as a power series in β up to nth order as well. Because these power series contain only first and higher order terms $[U_{ij}(\beta = 0) = 0]$ it is enough to substitute these series into the power series of G to obtain a power series of G in β up to nth order. Finally, we evaluate the average of each term in the power series.

Dyson's Eq. A5 is very suitable for obtaining a power series of G in the entries U_{ij}. G appears on both sides of the equation, but to obtain the power series of G up to nth order it is enough to substitute only terms up to $(n-1)$st order on the right hand side because each term is still multiplied by some entry U_{ij}. In particular, to obtain the first order terms of the power series, G may be replaced by G_0.

The power series of a particular entry (e.g., G_{00}) of the matrix G can now be found by expanding the matrix multiplication in Dyson's equation. However, we have to consider that only the off-diagonal entries of U are independent and the diagonal entries have to be replaced by $U_{jj} = -\sum_{i \neq j} U_{ij}$. Thus

$$\begin{aligned} G_{00} &= G^0_{00} + \sum_{i,j} G^0_{0i}U_{ij}G^0_{j0} + O(\beta^2) \\ &= G^0_{00} + \sum_{i \neq j} G^0_{0i}U_{ij}G^0_{j0} + \sum_{j} G^0_{0j}U_{jj}G^0_{j0} + O(\beta^2) \\ &= G^0_{00} + \sum_{i \neq j} (G^0_{0i} - G^0_{0j})\, G^0_{j0}U_{ij} + O(\beta^2). \end{aligned} \tag{C2}$$

In the following paragraphs we consider only the perturbation entries U_{ij} for nearest neighbors and assume that all other entries of U are zero. This is justified because the perturbations of rates to other pigments are not only small but also highly uncorrelated. We use Eq. IV1 to obtain U_{ij} and include the temperature dependence of the spectral overlap, by using $\sigma_h^2 = 8 \ln 2k_BTS = 8 \ln 2S/\beta$ from Eq. IV2. Furthermore, we want to correct for the temperature dependence of τ_{hop} as indicated in the text. Therefore we normalize G_{00} and U_{ij} by defining $\hat{G}_{00} = G_{00}/\tau_{hop}$ and $\hat{U}_{ij} = \tau_{hop}U_{ij}$. Note that Eq. C2 is also correct for these normalized values. We obtain

$$\begin{aligned} U_{ij} &= W(E_i, E_j, a) - \tau_{hop}^{-1} \\ &= \tau_{hop}^{-1}\left\{ \exp\left[\frac{1}{2}\beta(E_i - E_j)\right]\exp\left[-\frac{1}{4S}\beta(E_i - E_j)^2\right] - 1\right\} \\ \Rightarrow \hat{U}_{ij} &= \tau_{hop}U_{ij} = \left[\frac{1}{2}(E_i - E_j) - \frac{1}{4S}(E_i - E_j)^2\right]\beta + O(\beta^2). \end{aligned} \tag{C3}$$

We can now substitute this result in Eq. C2 and calculate the average but the result simplifies because the E_i are distributed independently. Therefore $\langle E_i - E_j\rangle = \langle E_i\rangle - \langle E_j\rangle = 0$ because $\langle E_i\rangle = \langle E_j\rangle$ and $\langle (E_i - E_j)^2\rangle = 2(\langle E_i^2\rangle - \langle E_i\rangle^2) = \sigma_{inh}^2/4 \ln 2$ so that

$$\langle \hat{U}_{ij}\rangle = -\left[\frac{\beta\sigma_{inh}^2}{16 \ln 2S}\right] + O(\beta^2), \tag{C4}$$

and $\langle U_{ij} \rangle$ is therefore independent of i and j. By substituting this into Eq. C2 we obtain

$$\langle \hat{G}_{00} \rangle = \hat{G}^0_{00} - \left[\frac{\beta\sigma^2_{inh}}{16 \ln 2S}\right] \sum_{j \in i+\Omega} (\hat{G}^0_{0i} - \hat{G}^0_{0j})\hat{G}^0_{j0} + O(\beta^2). \quad \text{(C5)}$$

Where Ω is the set of nearest neighbors of the pigment at site 0 so that $i+\Omega$ is the set of nearest neighbors of site i. The result may be further evaluated by considering the symmetry of G^0, i.e., $G^0_{i,j} = G^0_{0,j-i}$ and $G^0_{ij} = G^0_{ji}$. By rearranging the terms in this way

$$\begin{aligned}
\therefore &= \hat{G}^0_{00} - \left[\frac{\beta\sigma^2_{inh}}{16 \ln 2S}\right] \sum_{j \in i+\Omega} [\hat{G}^0_{0i}\hat{G}^0_{j0} - (\hat{G}^0_{j0})^2] + O(\beta^2) \\
&= \hat{G}^0_{00} - \left[\frac{\beta\sigma^2_{inh}}{16 \ln 2S}\right] \frac{1}{2} \sum_{j \in i+\Omega} [2\hat{G}^0_{0i}\hat{G}^0_{j0} - (\hat{G}^0_{0i})^2 - (\hat{G}^0_{0j})^2] + O(\beta^2) \\
&= \hat{G}^0_{00} + \left[\frac{\beta\sigma^2_{inh}}{16 \ln 2S}\right] \frac{1}{2} \sum_{j \in i+\Omega} (\hat{G}^0_{0i} - \hat{G}^0_{0j})^2 + O(\beta^2) \\
&= \hat{G}^0_{00} + \left[\frac{\beta\sigma^2_{inh}}{16 \ln 2S}\right] \frac{1}{2} \sum_{\substack{i \\ a \in \Omega}} (\hat{G}^0_{0i} - \hat{G}^0_{ai})^2 + O(\beta^2).
\end{aligned} \quad \text{(C6)}$$

Because only squares occur in the expression, we see that for any type of LHA, $\langle G_{00} \rangle$ increases with decreasing temperature.

The power series can be continued up to second order and the result is

$$\begin{aligned}
\langle \hat{G}_{00} \rangle = \hat{G}^0_{00} &+ \left[\frac{\beta\sigma^2_{inh}}{16 \ln 2S}\right] \frac{1}{2} \sum_{i,a \in \Omega} (\hat{G}^0_{0i} - \hat{G}^0_{ai})^2 \\
&+ \left[\frac{\beta\sigma_{inh}}{32 \ln 2}\right]^2 \left[-\sum_{i,a \in \Omega} (\hat{G}^0_{0i} - \hat{G}^0_{ai})^2 + \sum_{i,a,b \in \Omega} (\hat{G}^0_{00} - \hat{G}^0_{ab})(\hat{G}^0_{ai} - \hat{G}^0_{bi})^2\right] \\
&+ \left[\frac{\beta\sigma^2_{inh}}{16 \ln 2S}\right]^2 \left[\sum_{i,k,a,b \in \Omega} (\hat{G}^0_{0i} - \hat{G}^0_{ai})(\hat{G}^0_{0k} - \hat{G}^0_{bk})(\hat{G}^0_{0,k-1} - \hat{G}^0_{a,k-1})\right. \\
&\quad + \frac{1}{2} \sum_{i,a,b \in \Omega} (\hat{G}^0_{00} - \hat{G}^0_{0a} + \hat{G}^0_{ab})(\hat{G}^0_{0i} - \hat{G}^0_{ai}) \\
&\quad \cdot (\hat{G}^0_{0i} - \hat{G}^0_{bi}) - \frac{3}{4} \sum_{i,a \in \Omega} (\hat{G}^0_{0i} - \hat{G}^0_{ai})^2 \\
&\quad \left. + \sum_{i,a \in \Omega} \left(\hat{G}^0_{0i} - \hat{G}^0_{ai}\right)^2 (\hat{G}^0_{00} - \hat{G}^0_{0a})\right] + O(\beta^3).
\end{aligned} \quad \text{(C7)}$$

Unfortunately this expression contains terms with varying signs. Therefore it is hard to determine whether the second order terms will be positive or negative.

The perturbation of $\langle G_{00} \rangle$ is readily evaluated in particular cases because the matrix G^0 refers to the homogeneous LHA for which the master equation can be solved. For example in the case of an LHA system with 3×3 square units, for all nearest neighbours j of i: $G^0_{ij} = G^0_{00} - 2\tau_{hop}/9$ at least for λ close enough to 0 (see Eq. A4), while for all non-nearest neighbors k of i the $G^0_{ik} = G^0_{00} - 5\tau_{hop}/18$. This is sufficient to evaluate Eq. C5

$$\begin{aligned}
\frac{\langle G_{00} \rangle}{\tau_{hop}} &= \frac{G^0_{00}}{\tau_{hop}} + 0.22\left[\frac{\beta\sigma^2_{inh}}{16 \ln 2S}\right] + 0.001[\beta\sigma_{inh}]^2 + 0.13\left[\frac{\beta\sigma^2_{inh}}{16 \ln 2S}\right]^2 + O(\beta^3) \\
&= \frac{G^0_{00}}{\tau_{hop}} + 0.11\left[\frac{\sigma_{inh}}{\sigma_h}\right]^2 + 0.001[\beta\sigma_{inh}]^2 + 0.03\left[\frac{\sigma_{inh}}{\sigma_h}\right]^4 + O(\beta^3).
\end{aligned} \quad \text{(C8)}$$

Where we have obtained the second equality by substituting again that: $\sigma^2_h = 8 \ln 2S/\beta$. In a seven pigment hexagonal lattice, all six $j \neq i$ are nearest neighbours to i and $G^0_{ij} = G^0_{00} - \tau_{hop}/7$. In that case:

$$\begin{aligned}
\frac{\langle G_{00} \rangle}{\tau_{hop}} &= \frac{G^0_{00}}{\tau_{hop}} + 0.12\left[\frac{\beta\sigma^2_{inh}}{16 \ln 2S}\right] - 0.003[\beta\sigma_{inh}]^2 + 0.05\left[\frac{\beta\sigma^2_{inh}}{16 \ln 2S}\right]^2 + O(\beta^3) \\
&= \frac{G^0_{00}}{\tau_{hop}} + 0.06\left[\frac{\sigma_{inh}}{\sigma_h}\right]^2 - 0.009[\beta\sigma_{inh}]^2 + 0.01\left[\frac{\sigma_{inh}}{\sigma_h}\right]^4 + O(\beta^3).
\end{aligned} \quad \text{(C9)}$$

In both cases, the third term, that originates from the Boltzmann factor, has negligible influence unless $2S \gg \sigma_{inh}$. In both cases, the perturbation is positive so that $\langle G_{00} \rangle$ increases with decreasing temperature.

This result can be used in combination with Eq. B6 to appreciate the perturbation of τ_{mig} by the spectral inhomogeneity. Because the first order perturbation is zero, a_1 can be substituted by its average value $1/N$.

REFERENCES

Agranovich, V. M., and M. D. Galanin. 1982. Electron Excitation Energy Transfer in Condensed Matter. North-Holland, Amsterdam, 371 pp.

Bakker, J. G. C., R. van Grondelle, and W. T. F. den Hollander. 1983. Trapping, loss and annihilation of excitations in photosynthetic systems. II. Experiments with the purple bacteria *Rhodospirillum rubrum* and *Rhodopseudomonas capsulata*. *Biochim. Biophys. Acta.* 725:508–518.

Bay, Z., and R. M. Pearlstein. 1963. A theory of energy transfer in the photosynthetic unit. *Proc. Nat. Acad. Sci. USA.* 50:1071–1078.

Bergström, H., R. van Grondelle, and V. Sundström. 1989. Characterization of excitation energy trapping in photosynthetic purple bacteria at 77K. *FEBS Lett.* 250:503–508.

Borisov, A. Yu., R. Gadonas, R. V. Danielius, A. S. Piskarskas, and A. P. Razjivin. 1982. Minor component B-905 of light-harvesting antenna in *Rhodospirillum rubrum* chromatophores and the mechanism of singlet-singlet annihilation as studied by difference selective picosecond spectroscopy. *FEBS Lett.* 138:25–28.

Burshtein, A. I. 1985. Energy transfer kinetics in disordered systems. *J. Luminesc.* 34:167–188.

Danielius, R., and A. P. Razjivin. 1988. New data on the state of excitations in the light-harvesting antenna and their trapping by reaction centers. *In* Proc. of 5th UPS Meeting. Z. Rudzikas, A. Piskarskas, and R. Baltramiejunas, editors. World Scientific Co., Singapore. 231–239.

Deinum, G. 1991. Exciton migration in photosynthetic antenna systems. Ph.D. thesis, University of Leiden. 143 pp.

Deinum, G., T. J. Aartsma, R. van Grondelle, and J. Amesz. 1989. Singlet-singlet excitation annihilation measurements on the antenna of *Rhodospirillum rubrum* between 300 and 4K. *Biochim. Biophys. Acta.* 976:63–69.

Fetisova, Z. 1990. Excitation energy transfer in photosynthetic systems: pigment oligomerization effect. *In* Molecular Biology of Membrane-Bound Complexes in Phototrophic Bacteria. G. Drew, and E. A. Dawes, editors. Plenum Press, New York. 357–364.

Fleming, G. R., J. L. Martin, and J. Breton. 1988. Rates of primary electron transfer in photosynthetic reaction centres and their mechanistic implications. *Nature (Lond.)* 333:190–192.

Freiberg, A., V. I. Godik, T. Pullerits, and K. Timpmann. 1989. Picosecond dynamics of directed excitation transfer in spectrally heterogeneous light-harvesting antenna of purple bacteria. *Biochim. Biophys. Acta.* 973:93–104.

Freiberg, A., V. I. Godik, and K. Timpmann. 1987. Spectral dependence of the fluorescence lifetime of Rhodospirillum rubrum. Evidence for inhomogeneity of B880 absorption band. *In* Progress in Photosynthesis Research, Vol. 1. J. Biggins, editor. Martinus Nijhoff, Dortrecht. 45–48.

Gochanour, C. R., H. C. Andersen, and M. D. Fayer. 1979. Electronic excited state transport in solution. *J. Chem. Phys.* 70:4254–4271.

Godik, V. I., K. Timpmann, and A. Freiberg. 1988. Spectral inhomogeneity of the bacteriochlorophyll absorption band in *Rhodospirillum rubrum* obtained by fluorescence picosecond spectroscopy data. *Dokl. AN SSSR.* 298:1469–1473.

van Grondelle, R. 1985. Excitation energy transfer, trapping and annihilation in photosynthetic systems. *Biochim. Biophys. Acta.* 811:147–195.

van Grondelle, R., H. Bergström, V. Sundström, R. J. van Dorssen, M. Vos, and C. N. Hunter. 1988. Excitation energy transfer in the light-harvesting antenna of photosynthetic purple bacteria: the role of the long-wavelength absorbing pigment B896. *In* Photosynthetic Light-Harvesting Systems. H. Scheer, and S. Schneider, editors. Walter de Gruyter & Co. Berlin. 519–530.

van Grondelle, R., H. Bergström, V. Sundström, and T. Gillbro. 1987. Energy transfer within the bacteriochlorophyll antenna of purple bacteria at 77K, studied by picosecond absorption recovery. *Biochim. Biophys. Acta.* 894:313–326.

den Hollander, W. T. F., J. G. C. Bakker, and R. van Grondelle. 1983. Trapping, loss and annihilation of excitations in a photosynthetic system. I. Theoretical aspects. *Biochim. Biophys. Acta.* 725:492–507.

Jean, J. M., Chi-Kin Chan, G. R. Fleming, and T. G. Owens. 1989. Excitation transport and trapping on spectrally disordered lattices. *Biophys. J.* 56: 1203–1215.

Johnson, S. G., D. Tang, R. Jankowiak, J. M. Hayes, G. J. Small, and D. M. Tiede. 1989. Structure and marker mode of the primary electron donor state absorption of photosynthetic bacteria: hole-burned spectra. *J. Phys. Chem.* 93:5953–5957.

Källebring, B., and Ö. Hansson. 1991. A theoretical study of the effect of charge recombination on the transfer and trapping of excitation energy in photosynthesis. *Chem. Phys.* 149:361–372.

Karukstis, K. K. 1991. Chlorophyll fluorescence as a physiological probe of the photosynthetic apparatus. *In* Chlorophylls. H. Scheer, editor. CRC Press, Boca Raton, FL. 769–795.

Kleinherebrink, F. A. M., G. Deinum, S. C. M. Otte, A. J. Hoff, and J. Amesz. 1992. Energy transfer from long-wavelength absorbing antenna bacteriochlorophylls to the reaction center. *Biochim. Biophys. Acta.* 1099:175–181.

Knox, R. 1977. Photosynthetic efficiency and exciton transfer and trapping. *In* Topics in Photosynthesis. Vol. 2, J. Barber, editor. Elsevier, Amsterdam. 55–97.

Knox, R., and S. Lin. 1988. Time resolution and kinetics of "F680" at low temperature in spinach chloroplasts. *In* Photosynthetic Light-Harvesting Systems. Organization and Function. H. Scheer, and S. Schneider, editors. Walter de Gruyter & Co., Berlin. 567–577.

Kramer, H., L. Pennoyer, R. van Grondelle, W. Westerhuis, R. Niedermann, and J. Amesz. 1984. Low temperature optical properties and pigment organization of the B875 light-harvesting bacteriochlorophyll protein complex of purple photosynthetic bacteria. *Biochim. Biophys. Acta.* 767: 335–344.

Kudzmauskas, S., V. Liuolia, G. Trinkunas, and L. Valkunas. 1985. Nonlinear phenomena in chromatophores of photosynthetic bacteria excited by picosecond laser pulses. *Phys. Lett.* 111A:378–381.

Kudzmauskas, S., V. Liuolia, G. Trinkunas, and L. Valkunas. 1986. Minor component of the difference absorption spectra of photosynthetic bacteria chromatophores and nonlinear effects during excitation. *FEBS Lett.* 194: 205–209.

Kudzmauskas, S., V. Liuolia, G. Trinkunas, and L. Valkunas. 1988. Nonlinear phenomena in picosecond spectroscopy of photosynthetic membranes. *In* Proceedings of UPS Meeting Z. Rudzikas, A. Piskarskas, and R. Baltramiejunas, editors. World Scientific Co., Singapore. 248–256.

Kudzmauskas, S., L. Valkunas, and A. Yu. Borisov. 1983. A theory of excitation transfer in photosynthetic units. *J. Theor. Biol.* 105:13–23.

Lyle, P. A., and W. S. Struve. 1991. Temperature dependence of antenna excitation transport in native photosystem I particles. *J. Phys. Chem.* 95:4152–4158.

Martin, J.-L., J. Breton, A. J. Hoff, A. Migus, and A. Antonetti. 1986. Femtosecond spectroscopy of electron transfer in the reaction center of the photosynthetic bacterium *Rhodopseudomonas sphaeroides* R-26: direct electron transfer from the dimeric bacteriochlorophyll primary donor to the bacteriopheophytin acceptor with a time constant of 2.8 ± 0.2 psec. *Proc. Nat. Acad. Sci. USA.* 83:957–961.

Meckenstock, R. U., K. Kruche, R. A. Brunisholz, and H. Zuber. 1992. The light-harvesting core-complex and the B820-subunit from *Rhodopseudomonas marina*. Part II. Electron microscopic characterization. *FEBS Lett.* 311:135–138.

Meiburg, R. F. 1985. Orientation of components and vectorial properties of photosynthetic reaction centers. Ph.D. thesis. University of Leiden. 105 pp.

Miller, K. R. 1982. Three-dimensional structure of a photosynthetic membrane. *Nature (Lond.).* 300:53–55.

van Mourik, F., J. R. van der Oord, K. J. Visscher, P. S. Parkes-Loach, P. A. Loach, R. W. Visschers, and R. van Grondelle. 1991. Exciton interaction in the light-harvesting antenna of photosynthetic bacteria studied with triplet-singlet spectroscopy and singlet-triplet annihilation on the B820 subunit form of *Rhodospirillum rubrum*. *Biochim. Biophys. Acta.* 1059:111–119.

van Mourik F., Visschers R. W., and R. van Grondelle. 1992. Energy transfer and aggregate size effects in the inhomogeneously broadened core light-harvesting complex of *Rhodobacter sphaeroides*. *Chem. Phys. Lett.* 193:1–7.

van Mourik, F., K. J. Visscher, J. M. Mulder, and R. van Grondelle. 1993. Spectral inhomogeneity of the light-harvesting antenna of *Rhodospirillum rubrum* probed by T-S spectroscopy and singlet-triplet annihilation at low temperatures. *Photochem. Photobiol.* 57:19–23.

Movaghar, B., M. Grunewald, B. Ries, H. Bassler, and D. Wurtz. 1986. Diffusion and relaxation of energy in disordered organic and inorganic materials. *Phys. Rev. B.* 33:5545–5554.

Otte, S. C. M., F. A. M. Kleinherenbrink, and J. Amesz. 1993. Energy transfer between the reaction center and antenna in purple bacteria. *Biochim. Biophys. Acta.* 1143:84–90.

Osad'ko, I. S. 1979. Determination of electron-phonon coupling from structured optical spectra of impurity centers. *Sov. Phys. Usp.* 22: 311–329.

Paillotin, G., C. E. Swenberg, J. Breton, and N. E. Geacintov. 1979. Analysis of picosecond laser-induced fluorescence phenomena in photosynthetic membranes utilizing a master equation approach. *Biophys. J.* 25: 513–534.

Parson, R. P., and R. Kopelman. 1985. A self-consistent theory of non-equilibrium excitation transport in energetically disordered systems. *J. Chem. Phys.* 82:3692–3704.

Pearlstein, R. M. 1982. Excitation migration and trapping in photosynthesis. *Photochem. Photobiol.* 35:835–844.

Pearlstein, R. M. 1992. Kinetics of exciton trapping by monocoordinate reaction centers. *J. Luminescence.* 51:139–147.

Pullerits, T., and A. Freiberg. 1991. Picosecond fluorescence of simple photosynthetic membranes: Evidence of spectral inhomogeneity and directed energy transfer. *Chem. Phys.* 149:409–418.

Pullerits, T., and A. Freiberg. 1992. Kinetic model of primary energy transfer and trapping in photosynthetic membranes. *Biophys. J.* 63:879–896.

Robinson, G. W. 1967. Excitation transfer and trapping in photosynthesis. *Brookhaven Symp. Biol.* 19:16–48.

Rijgersberg, C., R. van Grondelle, and J. Amesz. 1980. Energy transfer and bacteriochlorophyll fluorescence in purple bacteria at low temperature. *Biochim. Biophys. Acta.* 592:53–64.

Seely, G. R. 1973. Effects of spectral variety and molecular orientation on energy trapping in the photosynthetic unit: a model calculation. *J. Theor. Biol.* 40:173–187.

Shimada, K., M. Mimuro, N. Tamai, and I. Yamazaki. 1989. Excitation energy transfer in *Rhodobacter sphaeroides* analyzed by the time resolved fluorescence spectroscopy. *Biochim. Biophys. Acta.* 975:72–79.

Shipman, L. L. 1980. Excitation migration in photosynthetic systems on the picosecond timescale. *Photochem. Photobiol.* 31:157–167.

Skala, L., and P. Jungwirth. 1989. Theory of excitation energy transfer in the primary processes of photosynthesis II. Group symmetry analysis of the bacterial light-harvesting complex. *Chem. Phys.* 137:93–98.

Skala, L., and V. Kapsa. 1989. Theory of excitation energy transfer in the primary processes of photosynthesis I. General results. *Chem. Phys.* 137: 77–92.

Sundström, V., R. van Grondelle, H. Bergström, E. Åkesson, and T. Gillbro. 1986. Excitation energy transport in the bacteriochlorophyll antenna systems of *Rhodospirillum rubrum* and *Rhodobacter sphaeroides*, studied by low-intensity picosecond absorption spectroscopy. *Biochim. Biophys. Acta.* 851:431–446.

Timpmann, K., A. Freiberg, and V. I. Godik. 1991. Picosecond kinetics of light excitation in photosynthetic purple bacteria in the temperature range 300–4K. *Chem. Phys. Lett.* 182:617–622.

Timpmann, K., F. G. Zhang, A. Freiberg, and V. Sundström. 1993. Detrapping of excitation energy from the reaction centre in the photosynthetic purple bacterium *Rhodospirillum rubrum*. *Biochim. Biophys. Acta.* 1183:185–193.

Trinkunas, G., and L. Valkunas. 1989. Exciton-exciton annihilation in picosecond spectroscopy of molecular systems. *Exp. Tech. Physik.* 37:455–458.

Valkunas, L. 1986. Influence of structural heterogeneity on energy migration in photosynthesis. *Laser Chem.* 6:253–267.

Valkunas, L. 1989. Nonlinear processes in picosecond spectroscopy of photosynthetic systems. *In* Proceedings 5th School on Quantum Electronics "Lasers—Physics and Applications." A. Y. Spasov, editor. World Scientific Co., Singapore. 541–560.

Valkunas, L., S. Kudzmauskas, and V. Liuolia. 1986. Noncoherent migration of exciton in impure molecular structures. *Sov. Phys.-Coll. (Liet. Fiz. Rink.).* 26:1–11.

Valkunas, L., V. Liuolia, and A. Freiberg. 1991. Picosecond processes in chromatophores at various excitation intensities. *Photosynth. Res.* 27: 83–95.

Visscher, K. J., H. Bergström, V. Sundström, C. N. Hunter, and R. van

Grondelle. 1989. Temperature dependence of energy transfer from the long wavelength antenna Bchl-896 to the reaction center in *Rhodospirillum rubrum, Rhodobacter sphaeroides* (w.t. and M21 mutant) from 77K to 177K, studied by picosecond absorption spectroscopy. *Photosynth. Res.* 22:211–217.

Visschers, R. W., M. C. Chang, F. van Mourik, P. S. Parkes-Loach, B. A. Heller, P. A. Loach, and R. van Grondelle. 1991. Fluorescence polarization and low-temperature absorption spectroscopy of a subunit form of light-harvesting complex I from purple bacteria. *Biochemistry.* 30: 5734–5742.

Visschers, R. W., F. van Mourik, R. Monshouwer, and R. van Grondelle. 1993. Inhomogeneous spectral broadening of the B820 subunit form of LH1. *Biochim. Biophys. Acta.* 1141:238–244.

Vos, M., R. van Grondelle, F. W. van der Kooij, D. van de Poll, J. Amesz, and L. N. M. Duysens. 1986. Singlet-singlet annihilation at low temperatures in antenna of purple bacteria. *Biochim. Biophys. Acta.* 850:501–512.

Wang, R. T., and R. K. Clayton. 1971. The absolute yield of bacteriochlorophyll fluorescence in vivo. *Photochem. Photobiol.* 13:215–224.

Werst, M., Y. Jia, L. Mets, and G. R. Fleming. 1992. Energy transfer and trapping in the photosystem I core antenna: A temperature study. *Biophys. J.* 61:868–878.

Wittmershaus, B. P. 1987. Measurements and kinetic modelling of picosecond time-resolved fluorescence from photosystem I and chloroplasts. *In* Progress in Photosynthesis Research. Vol. 1. J. Biggins, editor. Martinus Nijhoff, Dordrecht. 75–82.